INL/EXT-14-32505
Rev: 0

NEET In-Pile Ultrasonic Sensor Enablement-Final Report

J. Daw, J. Rempe, J. Palmer (INL)
P. Ramuhalli, P. Keller, R. Montgomery (PNNL)
H.T. Chien (ANL)
B. Tittmann, B. Reinhardt (PSU)

September 2014

The INL is a U.S. Department of Energy National Laboratory
operated by Battelle Energy Alliance

INL/EXT-14-32505
Rev: 0

NEET In-Pile Ultrasonic Sensor Enablement-Final Report

J. Daw

J. Rempe

J. Palmer

P. Ramuhalli

P. Keller

R. Montgomery

HT Chien

B. Tittmann

B. Reinhardt

September 2014

Idaho National Laboratory
Idaho Falls, Idaho 83415

Prepared for the
U.S. Department of Energy
Office of Nuclear Energy, Science, and Technology
Under DOE Idaho Operations Office
Contract DE-AC07-05ID14517

This page intentionally left blank.

EXECUTIVE SUMMARY

Several programs funded by the Department of Energy Office of Nuclear Energy (DOE-NE), such as the Fuel Cycle Research and Development, Advanced Reactor Concepts, Light Water Reactor Sustainability, and Next Generation Nuclear Plant programs, are investigating new fuels and materials for advanced and existing reactors. A key objective of such programs is to understand the performance of these fuels and materials during irradiation. The Nuclear Energy Enabling Technology (NEET) Advanced Sensors and Instrumentation (ASI) in-pile instrumentation development activities are focused upon addressing cross-cutting needs for DOE-NE irradiation testing by providing higher fidelity, real-time data, with increased accuracy and resolution from smaller, compact sensors that are less intrusive.

Ultrasonic technologies offer the potential to measure a range of parameters during irradiation of fuels and materials, including geometry changes, temperature, crack initiation and growth, gas pressure and composition, and microstructural changes under harsh irradiation test conditions. There are two primary issues that currently limit in-pile deployment of ultrasonic sensors. The first is transducer survivability. The ability of ultrasonic transducer materials to maintain their useful properties during an irradiation must be demonstrated. The second issue is signal processing. Ultrasonic testing is typically performed in a lab or field environment, where the sensor and sample are accessible. The harsh nature of in-pile testing and the variety of desired measurements demand that an enhanced signal processing capability be developed to make in-pile ultrasonic sensors viable. To address these issues, the NEET ASI program funded a three year Ultrasonic Transducer Irradiation and Signal Processing Enhancements project, which was completed as a collaborative effort between the Idaho National Laboratory, the Pacific Northwest National Laboratory, the Argonne National Laboratory, and the Pennsylvania State University. The objective of this report is to document the objectives and accomplishments from this three year project. As summarized within this document, significant work has been accomplished during this three year project:

- ***Transducer Irradiation Test*** - The first task of this project supports efforts to develop a test capsule design and define irradiation conditions for evaluating the most promising candidate piezoelectric and magnetostrictive transducer materials and designs. In July FY-12, the ATR NSUF announced that a PSU-led proposal for irradiating ultrasonic transducers was selected, and the irradiation would occur in the Massachusetts Institute of Technology Nuclear Research Reactor (MITR). Therefore, this NEET project leveraged ATR NSUF funding, allowing all of the planned accomplishments to be completed.

  FY-12 project efforts focused on developing a capsule design and on identifying appropriate test conditions, identifying transducers for inclusion in the capsule, appropriate post-irradiation examinations, and identifying out-of-pile laboratory tests needed to support the irradiation. As documented in this report, the irradiation test builds on prior research; and conditions were designed to exceed previous tests in terms of the number of materials tested and accumulated fluence. The purpose of this test is to irradiate the most promising transducer materials to a total fast fluence of at least 1×10^{21} n/cm^2. This project selected suitable piezoelectric and magnetostrictive candidates identified based on material properties and previous research. Piezoelectric materials included in this irradiation are aluminum nitride (AlN), bismuth titanate niobate (Bi_3TiNbO_9), and zinc oxide (ZnO). Magnetostrictive materials included are Remendur and Galfenol.

  During FY-13, transducer design issues, such as electrical connections and transducer to sample coupling, were addressed. An updated test capsule design was developed that is capable of accommodating all test specimens as well as real time instrumentation for monitoring temperature and neutron and gamma flux. Transducers were fabricated and transported to MIT for installation in the irradiation test capsule and to PSU for out-of-pile furnace testing. Initial furnace testing was performed to evaluate the performance of transducers at expected test temperatures. Results confirmed that the transducer designs were sufficiently robust with respect to temperature. Further out-of-pile testing will be performed by PSU in FY-14 using ATR-NSUF funding.

During FY-14 representatives from INL (responsible for construction of magnetostrictive transducers) and PSU (responsible for construction of piezoelectric transducers) visited MIT and applied cable terminations to test transducers prior to installation in the irradiation test capsule. The test was installed in the MITR, and the irradiation began in February 2014. To date, the capsule has reached an integrated fast fluence (Energy>1.0MeV) of $4.1*10^{20}$ n/cm^2. As discussed within this report, two piezoelectric transducers and both magnetostrictive transducers are still operational. Two piezoelectric transducers failed during reactor start-up. Of the surviving piezoelectric transducers, the aluminum nitride transducer has performed well during periods of steady reactor operation and appears to be a good candidate for in-core applications. The bismuth titanate transducer showed steady deterioration of signal strength during start-up and the first full reactor cycle, but has recovered during subsequent cycles (with increased reactor power). Both magnetostrictive transducers exhibited stable performance over the first reactor cycle, with gradual degradation observed for subsequent cycles. The Galfenol transducer has shown less degradation than the Remendur transducer, but degradation in both cases is small enough that both should be considered good candidates for in-core applications.

- ***Signal Processing Enhancement*** **-** The second task of this project addresses the need for an enhanced signal processing capability for future in-pile ultrasonic measurements. Initial project efforts were focused on a background survey of existing methodologies and development of the signal processing requirements associated with ultrasonic signals applied to in-core applications. Then, representative ultrasonic thermometry data was produced by INL and transmitted to PNNL and ANL for use in developing signal processing algorithms. As discussed within this report, PNNL focused on statistical analysis of the signals and comparison of methods to improve signal to noise ratio. ANL focused on application of signal processing methods using a software package developed for this task.

  Results indicate that time-domain processing produces the best estimate of temperature resolution, though only slightly better than frequency or time-frequency based analysis methods. Time resolution was generally found to be within a range of 1-2%, producing a sound velocity resolution of approximately 100 m/s. Due to the limited data set, temperature resolution was estimated to be 46°C based on one standard deviation from mean. This resolution estimate can be improved with increased by using larger data sets for analysis. Demonstration of an automated data processing package was successful, but differences in velocities calculated from data collected for this effort and data collected during prior testing for the same material, with a different process history, indicate that ultrasonic thermometers must be calibrated individually. This will ensure that differences due to variations in materials and fabrication processes have minimal effect on measurement accuracy.

CONTENTS

FIGURES

TABLES

ACRONYMS

ANL	Argonne National Laboratory
ARC	Advanced Reactor Concepts
ASI	Advanced Sensors and Instrumentation
ATR	Advanced Test Reactor
BNC	Bayonet Neill-Concelman
BWR	Boiling Water Reactor
CANDU	CANada Deuterium Uranium
CEA	Commissariat à l'Énergie Atomique et aux Energies Alternatives
DOE	Department of Energy
DOE-NE	Office of Nuclear Energy in the Department of Energy
ENDF	Evaluated Nuclear Data Files
FCRD	Fuel Cycle Research and Development
FFT	Fast Fourier Transform
HFIR	High-Flux Isotope Reactor
HTIR-TC	High Temperature Irradiation Resistant ThermoCouple
ID	Inner Diameter
INL	Idaho National Laboratory
JHR	Jules Horowitz Reactor
LVDT	Linear Variable Differential Transformer
LWR	Light Water Reactor
LWRS	Light Water Reactor Sustainability
MIT	Massachusetts Institute of Technology
MITR	Massachusetts Institute of Technology Nuclear Research Reactor
MTR	Material Test Reactor
NEET	Nuclear Energy Enabling Technologies
NDE	Nondestructive Evaluation
NDT	Nondestructive Testing
NGNP	Next Generation Nuclear Plant
NSUF	National Scientific User Facility
OD	Outer Diameter
ORNL	Oak Ridge National Laboratory
PIE	Post-Irradiation Examination
PNNL	Pacific Northwest National Laboratory
PWR	Pressurized Water Reactor
SFR	Sodium Fast Reactor
SNR	Signal to Noise Ratio
UT	Ultrasonic Thermometer
TRISO	Tri-structural Isotropic

1. INTRODUCTION

Ultrasonic technologies offer the potential to measure a range of parameters, including geometry changes, temperature, crack initiation and growth, gas pressure and composition, and microstructural changes, under harsh irradiation test conditions. Many Department of Energy-Office of Nuclear Energy (DOE-NE) programs would benefit from the use of ultrasonic technologies to provide enhanced sensors for in-pile instrumentation during irradiation testing. For example, the ability of single, small diameter ultrasonic thermometers (UTs) to provide a temperature profile in candidate metallic and oxide fuel. Other ultrasonic methods, such as sensors to measure released fission gas pressure and composition, could clearly benefit future irradiations.[1]

It is recognized that if reliable ultrasonic transducers can be deployed in-pile, measurement accuracies may be considerably enhanced. In addition, ultrasound-based sensors offer the potential for significant reductions in irradiation capsule size. It is currently anticipated that some ultrasound-based sensor applications under investigation require high frequency piezoelectric transducers, which have previously been observed to suffer rapid degradation when exposed to neutron radiation. Another technology deployment issue common to many ultrasonic measurement techniques is the need for enhanced signal processing techniques, as the in-core environment is known to cause significant signal noise. This report documents results from a three year project established to address these two technology deployment issues.

1.1. Project Overview

Several DOE-NE programs, such as the Fuel Cycle Research and Development (FCRD),[1] Advanced Reactor Concepts (ARC),[2,3] Light Water Reactor Sustainability (LWRS),[4] and Next Generation Nuclear Plant (NGNP) [5 - 11] programs, are investigating new fuels and materials for advanced and existing reactors. A key objective of such programs is to understand the performance of these fuels and materials during irradiation. Nuclear Energy Enabling Technology (NEET) Advanced Sensors and Instrumentation (ASI) in-pile instrumentation development activities are focused upon addressing cross-cutting needs for DOE-NE irradiation testing by providing higher fidelity, real-time data, with increased accuracy and resolution from smaller, compact sensors that are less intrusive.[12]

The NEET ASI established the three-year Ultrasonics Transducer Irradiation and Signal Processing Enhancements project to enable in-core use of ultrasound-based sensors that are uniquely capable of meeting DOE program enhanced instrumentation needs. This project consists of two tasks, one to evaluate ultrasound transducer survivability and one to evaluate methods to enhance signal processing.

The objective for Task 1 of this project is to evaluate the performance of ultrasonic transducer materials in high flux/high temperature irradiation environments. This project leverages results from an ATR NSUF-funded PSU-led MITR irradiation and supports an irradiation evaluation of the most promising candidate piezoelectric and magnetostrictive transducer materials. Building upon recent results from ultrasonic sensor investigations, an in-depth review of prior piezoelectric and magnetostrictive transducer irradiations was used to develop a list of candidate materials for irradiation evaluation. In addition, a design for an instrumented-lead irradiation test capsule and a test plan for evaluating ultrasonic transducer materials were developed. This irradiation is classified as an instrumented lead test, such that real time signals are received from the transducers. Such a test enables an accurate measure of the performance and possible degradation of candidate transducer materials under irradiation. This test also provides fundamental data on piezoelectric and magnetostrictive material performance in irradiation environments. Prior tests either tested too few samples, or samples that were too dissimilar, for such a comparison. This additional information may enable further application of ultrasonic technologies in the future.

The objective for Task 2 is to enhance signal processing methods used to support various types of ultrasonic sensors. Ultrasonic instrumentation is a well-developed technology widely used in non-nuclear appli-

cations; however, several improvements are required for successful implementation in irradiation tests. The harsh testing conditions that ultrasonic sensors must survive are likely to reduce signal to noise ratios, complicating identification of signal features. Therefore, a primary goal of Task 2 work is the development of methods to improve signal to noise ratio. Ultrasonic sensors utilize several different signal characteristics (i.e. delay time, resonant frequency, attenuation, etc.) for monitoring the many parameters previously identified. Enhanced methods of processing these signal characteristics, specific for in-pile ultrasonic applications, were evaluated and demonstrated in Task 2 for use with an ultrasonic thermometry system, a representative ultrasonic sensor system of interest to DOE-NE programs.

1.2. Report Content and Organization

The objective of this report is to document final results of the Ultrasonic Transducer Irradiation and Signal Processing Enhancements project. Section 2 provides background information related to irradiation test conditions, typical ultrasound-based sensors, and the types of irradiation parameters and conditions of interest to DOE programs. Section 3 summarizes project efforts to support the PSU-led ultrasonic transducer material irradiation test, including a description of the irradiation test conditions, a discussion of the transducer materials and sensors included in the test, a description of the test capsule, and test results to date. Section 4 lists requirements for enhanced signal processing capabilities needed for future development of in-pile ultrasound based sensor systems, and documents the evaluation of a signal processing algorithm for use with ultrasonic thermometry data. Section 5 summarizes key accomplishments for this project. Section 6 lists references cited in this document.

Additional information on the motivation for this work, the process used in selecting candidate transducer materials, and preliminary designs of the test capsule and transducers, is available in the FY-12 status report.[13] The FY-13 status report contains detailed information on the final test capsule design.[14] The FY-13 status report also provides detailed information related to the design and fabrication processes of the test transducers and the test plan.

2. BACKGROUND

To ensure that NEET in-pile instrumentation research is relevant, sensor enhancements must be able to survive the irradiation conditions of interest to DOE-NE programs. It is also important that the enhanced sensors be able to measure thermal and structural properties and irradiation test parameters with the desired accuracy and resolution required by these DOE-NE programs. Ultrasound sensors offer unique capabilities to meet these in-pile measurement needs. This section summarizes information obtained from the various DOE-NE programs that guided NEET ultrasonic sensor investigations. This section describes representative fuel and materials and irradiation test conditions that are currently of interest to DOE-NE programs. In addition, selected ultrasound sensors are described to illustrate the unique capabilities of these sensors to meet DOE-NE program needs. Key phenomena of interest in fuel and materials performance evaluations are identified for which additional data are needed. Physical parameters that must be detected during irradiation tests are also listed with desired accuracies (specified by various DOE-NE programs).

2.1. Typical MTR Conditions for DOE-NE Irradiations

Most DOE-NE irradiations are performed in the Advanced Test Reactor (ATR) located at the Idaho National Laboratory (INL) and the High Flux Irradiation Reactor (HFIR) located at Oak Ridge National Laboratory (ORNL). This section provides a brief description of each of these reactors and typical irradiation options in each facility.

The ATR is a unique facility for scientific investigation of nuclear fuel and materials.[1,15] Designed to allow simulation of long neutron radiation exposures in a short time period, the ATR has a maximum power rating of 250 MW_{th} with a maximum unperturbed thermal neutron flux of 1 x 10^{15} n/cm^2-s and a maximum fast neutron flux of 5 x 10^{14} n/cm^2-s. The ATR is cooled by pressurized (2.5 MPa/360 psig) water that enters the reactor vessel bottom at an average temperature of 52 °C (126 °F), flows up outside cylindrical tanks that support and contain the core, passes through concentric thermal shields into the open part of the vessel, then flows down through the core to a flow distribution tank below the core. When the reactor is operating at full power, the primary coolant exits the vessel at 71 °C (160 °F).

The HFIR is a beryllium-reflected, pressurized, light-water-cooled and moderated flux-trap-type reactor. The core, which consists of aluminum-clad fuel plates, currently utilizes highly enriched ^{235}U fuel, with a design power level of 100 MW_{th}, a maximum thermal flux of 2 x 10^{15} n/cm^2 and a maximum fast flux of 1 x 10^{15} n/cm^2. The HFIR was originally designed (in the 1960s) to primarily support the overall program to produce transuranic isotopes for use in the U.S. heavy-element research program. Today, the reactor is a highly versatile machine, producing medical and transuranic isotopes and performing materials test experimental irradiations and neutron-scattering experiments, including the capability to conduct cold-source low-temperature neutron experiments.

The ATR and HFIR offer higher flux levels than most other MTRs. Although the high flux levels present in these MTRs are advantageous for accumulation of high fluence, there are questions related the applicability of their energy spectra for assessing sample performance in fast reactors and the effect of localized heating associated with the higher gamma fields present in such MTRs. The effects of some of these differences can be quantified using enhanced real-time in-pile instrumentation to obtain precise measurements of the flux as a function of energy level and of temperature increases associated with gamma heating. Several DOE-NE efforts, such as the ATR NSUF and the FCRD programs, are sponsoring sensor development efforts to make ATR and HFIR competitive with international MTRs using real-time instrumentation options by adding additional in-pile measurement capabilities required for US research programs. This NEET ultrasonics cross-cutting effort offers US MTRs additional in-pile instrumentation capabilities by enabling ultrasonics sensors that offer unprecedented measurement accuracy and resolution.

2.2. Potential Ultrasound Based Sensors for In-Core Use

To illustrate the benefits of ultrasound-based sensors, this section describes selected instrumentation that could be deployed in US MTRs using results from the current irradiation test and signal processing enhancement results.

2.2.1. Ultrasonic Thermometer

Ultrasonic thermometry has the potential to improve upon temperature sensors currently used for in-core temperature measurements.[16] Ultrasonic Thermometers (UTs) can be made with very small diameters while maintaining a high level of durability because the sensor consists of a small diameter rod (typical diameters range from 0.25 mm to 1 mm, although a sheath may be required for some environments).[17] In fact, a small diameter rod is desirable; ultrasonic wave dispersion is avoided when the rod diameter is sufficiently small compared to the acoustic wavelength.[18] Temperature sensors based on electrical measurements (i.e., thermocouples, thermistors, resistance thermometers, noise thermometers) are limited by the electrical shunting errors caused by degradation of the resistivity of electrical insulators when subjected to high temperatures (> 1800 °C). UT temperature measurements may potentially be made near the melting point of the sensor material, allowing temperatures in excess of 3000 °C to be monitored for certain sensor materials. A clear line of sight is not required with UTs, as is the case for most optical pyrometry applications. With proper selection of materials, UTs may be used in very harsh environments, such as high temperature steam or liquid metals. By introducing multiple acoustic discontinuities into the sensor, UTs are able to perform temperature measurements at several points along the sensor length, whereas thermocouples typically only allow measurement at a single location.

UTs work on the principle that the speed at which sound travels through a material (acoustic velocity) is dependant on the temperature of the material. Temperatures may be derived by introducing an acoustic pulse to the sensor and measuring the time delay of echoes. A conceptual design of a multi-segment UT, with key components identified, is shown in Figure 2-1. The magnetostrictive transducer generates a narrow ultrasonic pulse in the probe. The ultrasonic pulse propagates to the sensor wire, where a fraction of the pulse energy is reflected at each acoustic discontinuity. Each reflected pulse is received by the excitation coil, transformed into an electrical signal, amplified and evaluated through signal processing. The time interval between two adjacent echoes is evaluated and compared to a calibration curve to give the average temperature in the corresponding sensor segment. When a number of notches are available on the wire sensor, the various measurements give access to a temperature profile along the probe.

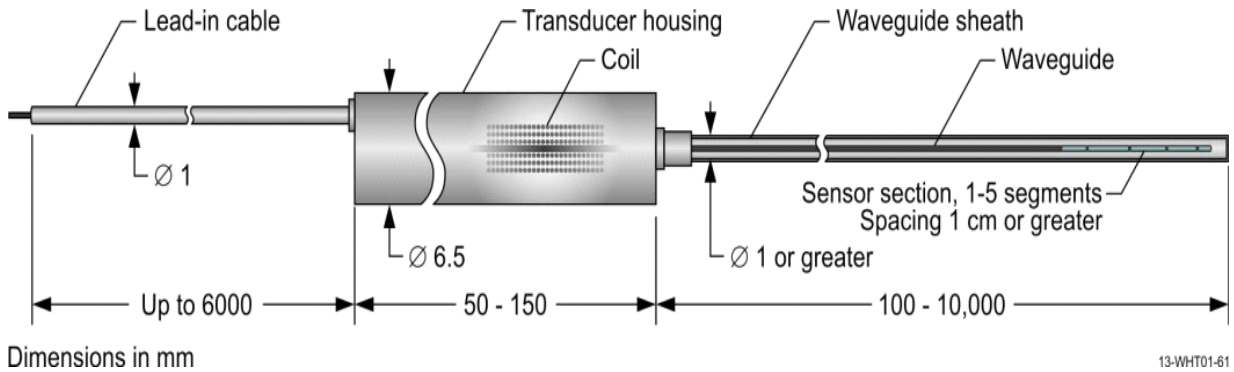

Figure 2-1. Schematic showing typical components of a UT and signal processing equipment.

Prior US UT applications demonstrated the viability of this technology for Light Water Reactor (LWR), High Temperature Gas Reactor (HTGR), and Sodium Fast Reactor (SFR) test conditions (see Fig-

ure 2-2).[19] However, prior in-pile applications were primarily limited to fuel damage tests that ceased several decades ago.[19] Although these tests clearly demonstrated the ability of UTs to withstand high temperatures (up to nearly 2900 °C), test durations were typically limited to less than 100 hours; and data acquisition was cumbersome due to the limitations of signal processing systems available at the time. The availability of new materials and signal processing techniques suggests that this technology could be ideally suited for irradiations that require robust, high accuracy, compact sensors.

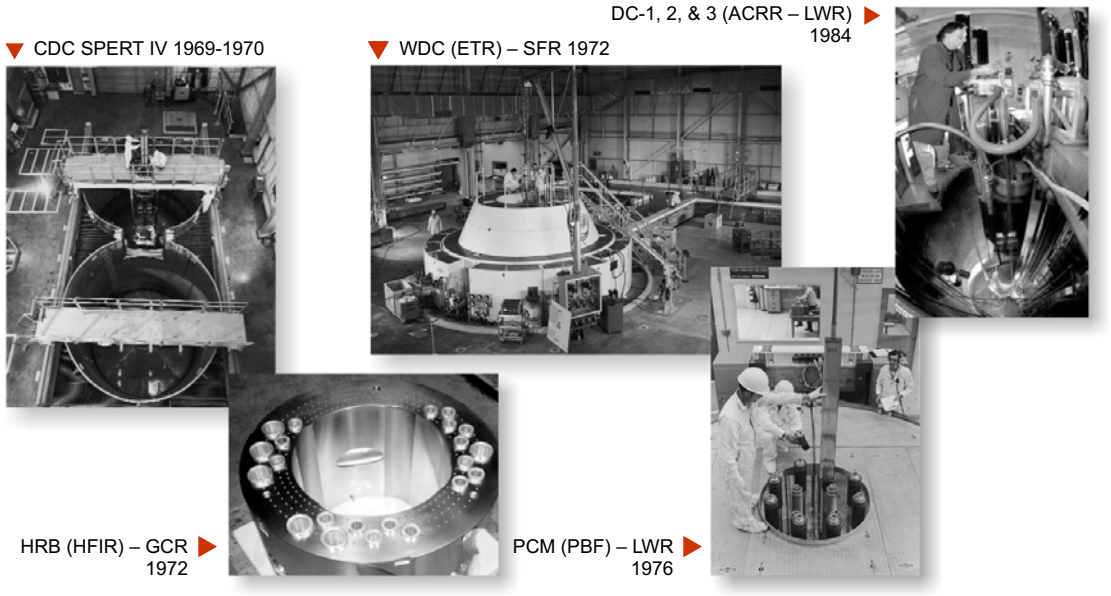

Figure 2-2. Prior UT in-pile applications in the US.

2.2.2. Acoustic Gas Monitor

A dedicated acoustic sensor containing a piezoelectric PZT (Lead Zirconate Titanate) transducer has been developed by the Commissariat à l'Énergie Atomique et aux Energies Alternatives (CEA) to measure fission gas release pressure and composition online in a fuel rod during irradiation experiments. Figure 2-3(a) illustrates some of the details related to the design of this acoustic fission gas release sensor.[20-28] This assembly is composed of a small cylindrical cavity containing the gas to be analyzed. The upper part of the cavity is closed by a thin stainless steel plate. The piezoelectric transducer is fixed on this plate, in order to generate and measure acoustic waves, through the plate, in the gas cavity. Wires are directly welded on the piezo-ceramics electrodes. Acoustic waves propagate in the gas inside the cavity (diameter 10 mm and length 12.5 mm) which is connected to the fuel rod plenum. The measurement of the reflected waves allows assessment of the acoustic impedance of this system [see Figure 2-3(b)]. The signal and its echoes are recorded, and the time-of-flight of the signal and its attenuation are measured. From these measurements, it is possible to deduce simultaneously the molar mass of the gas (from the acoustic wave velocity) and the pressure of the gas (from the attenuation of the echoes). The online assessment of these two parameters is then used to obtain information regarding the fraction of fission gases released in the fuel rod.

After laboratory testing of acoustic sensor prototypes was completed, its performance was evaluated at OSIRIS on a pre-irradiated high burnup mixed oxide PWR fuel rod in the 2010 REMORA-3 irradiation experiment. Instrumentation installed on this fuel rod included the acoustic gas sensor, a type C thermocouple, and an acoustic gas sensor. Results indicate that the PZT experienced degradation due to high fluences to which it was exposed (total gamma dose of 0.25 MGy, and thermal fluences of 3.5 x10^{17}n/cm^2).

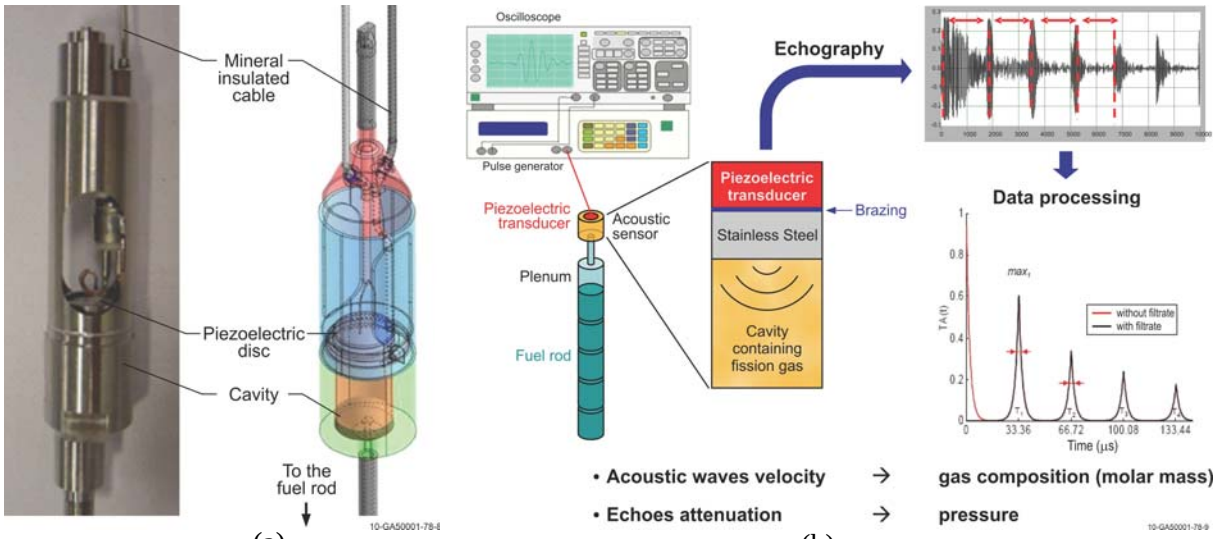

Figure 2-3. CEA fission gas pressure and composition detection (a) sensor and (b) system operation.

2.3. Fuels and Material Irradiations

Several DOE-NE programs, such as the FCRD,[1] ARC,[2,3a] LWRS,[4] and NGNP[5-7] programs, are investigating new fuels and materials for advanced and existing reactors. A key objective of such programs is to understand the performance of these fuels and materials when irradiated. The NEET ASI in-pile instrumentation development activities are focused upon addressing cross-cutting needs for DOE-NE irradiation testing by providing smaller, compact sensors that can provide higher fidelity, real-time data, with increased accuracy and resolution.[9] The NEET ASI funded the Ultrasonic Transducer Irradiation and Signal Processing Enhancements project to help enable the use of enhanced ultrasound-based sensors for irradiation testing. To ensure that NEET in-pile instrumentation research is relevant, these enhanced sensors must be able to survive the irradiation conditions of interest to DOE-NE programs. It is also important that the enhanced sensors be able to measure thermal and structural properties and irradiation test parameters with the desired accuracy and resolution required by these DOE-NE programs. This section summarizes information obtained from the various DOE-NE programs used to guide the NEET ultrasonic sensor investigations.

2.3.1. Fuels

DOE-NE efforts to develop and evaluate the performance of new fuels and cladding materials are conducted in the FCRD, LWRS, and NGNP programs. Hence, NEET research must produce sensors able to withstand the operating conditions of interest to these programs. It is also important that the enhanced sensors be able to measure test parameters with the desired accuracy and resolution required by these DOE-NE programs and that the sensors be compact to minimize their impact on irradiation test data. As discussed in Reference 13, fuel rods may be fabricated from ceramic or metallic materials. Particle fuel consists of ceramic materials encased in carbide coatings. Reference 13 also describes typical irradiation conditions and test configurations that are used by these DOE-NE programs.

In-situ instrumentation is desired to provide real-time data on fuel performance phenomena. Without wireless transmission capabilities, drop-in or static capsule experiments only allow data to be obtained at the

a. The ARC program is limiting current research to evaluating advanced structural materials and relies on other DOE-NE programs for fuel development.

endpoint of an experiment. In-situ instrumentation in irradiation tests can provide data showing the evolution of particular phenomena over time. Selected parameters of interest for fuel modeling, with accuracies currently requested by DOE-NE programs, are listed in Table 2-1.[11,12,29]

Table 2-1. Summary of desired parameters for detection during fuel irradiation tests.[a]

Parameter	Representative Peak Value	Desired	
		Accuracy	Spatial Resolution
fuel temperature	Ceramic LWR - 1400 °C	2%	1-2 cm (axially); 0.5 cm (radially)
	Ceramic SFR- 2600 °C		
	Metallic SFR - 1100 °C		
	TRISO HTGR -1250 °C		
cladding temperature	Ceramic LWR - <400 °C	2%	1-2 cm (axially)
	Ceramic SFR - 650 °C		
	Metallic SFR - 650 °C		
	TRISO GCFR	NA	NA
pressure in fuel rod plenum	Ceramic LWR - 5.5 MPa	5%	NA[b]
	Ceramic SFR-8.6 MPa		
	Metallic SFR - 8.6 MPa		
	HTGR-NA		
LWR, SFR, and HTGR fission gas release (amount and composition)	0-100% of inventory	10%	NA
LWR and SFR fuel and cladding dimensions (includes fuel / cladding gap size); HTGR- NA	Initial Length, 1 cm	1%	NA
	Outer diameter/Strain, 0.5 cm/5-10%	0.1%	NA
	Fuel-Cladding Gap (0-0.1 mm)	0.1%	NA
LWR, SFR, and HTGR fuel morphology/microstructure/ cracking/ constituent redistribution	Grain size,10 μm	5%	1-10 μm
	Swelling/Porosity, 5-20%	2%	
	Crack formation and growth	2%	10-100 μm
fuel thermal properties	Thermal conductivity Ceramic: < 8 W/mK; Metallic: < 50 W/mK; TRISO pebble/compact: 4-12 W/mK	4%	< 1 cm (radially)
	Density (inferred from changes in length, diameter, porosity, etc.) Ceramic: < 11 g/cm^3; Metallic: < 50 g/cm^3; TRISO pebble/compact: 2.25 g/cm^3[c]	2%	NA
maximum neutron flux for estimating fluence and fuel burnup for fuel irradiations	Thermal neutron flux - ~1-5 x 10^{14} n/cm^2-s	1-10%	5 cm (axially)
	Fast neutron flux (E> 1 MeV) - ~1-5×10^{14} n/cm^2-s	15%	5 cm (axially)

a. Representative peak values, accuracy, and resolution are based on engineering judgement by cognizant program experts.
b. NA-Not Applicable.
c. Value dependent upon particle packing fraction and matrix.

2.3.2. Materials

DOE-NE programs are also focused on degradation that may occur in high temperature alloys, vessel and internal materials, weldments, and graphite. The LWRS and NGNP programs are the only programs currently conducting materials irradiations. Other programs, such as the ARC program that relies on SFR technologies, have identified the need for and/or are planning materials irradiation tests. It should also be noted that many irradiation effects investigations are currently conducted out-of-pile using post irradiation examination (PIE) techniques. However, it is anticipated that the need to validate new computational tools for simulating material performance during irradiation will require higher fidelity data with increased accu-

racy and resolution. Such requirements demand that irradiations be performed in instrumented tests where data can be obtained real-time in the environment that exists during the irradiation (e.g., at representative temperatures, pressures, and fluxes).

Currently, most material irradiations rely on PIE to characterize material properties after an irradiation is completed. Enhanced in-pile instrumentation offers the potential for increased accuracy higher fidelity data since measurements are obtained at the conditions of interest. Selected parameters of interest for materials performance modeling, with currently-requested accuracies, are listed in Table 2-2.

Table 2-2. Summary of desired parameters for detection during materials irradiation tests.[a,b]

Parameter	Representative Peak Values	Desired	
		Accuracy	Spatial Resolution
Material temperature distribution	LWRS Fuel Cladding- >1200 °C	2%	1-2 cm (axially); 0.5 cm (radially)
	LWRS Vessel and Internal Materials- 500 °C		
	HTGR and LWRS high temperature alloys- 950 °C		
	HTGR Graphite - 600 to 1200 °C	± 50 °C (axially) ± 40 °C (radially)	NA[c]
Material dimensional changes due to swelling;	Initial Specimen Length, HTGR Graphite - 2.54 cm	1%	NA
	Outer diameter/Strain, LWR vessel and internal materials - 0.5 cm/5-10%	0.1%	NA
Material morphology/ microstructure/cracking/ constituent redistribution	Grain size, LWR vessel and internal materials > 10 μm	5%	1-10 μm
	Swelling/Porosity, LWR vessel and internal materials 5-20%	2%	10-100 μm
	Crack formation and growth LWR vessel and internal materials > 10 μm	2%	10-100 μm
Material thermal properties	Thermal conductivity HTGR Graphite -	4%	< 1 cm (radially)
	Thermal conductivity LWR vessel and internal materials ~50 W/m-K	5-20%	< 1 cm
	Thermal coefficient of expansion; HTGR Graphite - 5%	2%	NA
	Density (estimated from changes in length, diameter, porosity, etc.) HTGR Graphite - 0.5%	0.2%	NA
Material mechanical/electrical properties	Irradiation creep HTGR Graphite - 3-4%	NA	NA
	Young's modulus HTGR Graphite - 3-4%	NA	NA
	Electrical resistivity HTGR Graphite - 3-4%	NA	NA
	Poisson's ratio HTGR Graphite - 3-4%	NA	NA
	Fracture toughness, shear strength HTGR Graphite - 3-4%	NA	NA
Material irradiation neutron flux for estimating fluence	Thermal neutron flux - ~1-5 x 10^{14} n/cm^2-s	1-10%	5 cm (axially)
	Fast neutron flux (E> 1 MeV) - ~1-5×10^{14} n/cm^2-s	15%	5 cm (axially)

a. Representative peak values, accuracy, and resolution are based on engineering judgement and are preliminary.
b. Only LWRS and NGNP irradiation information available for a limited number of parameters at this time.
c. NA-Not Available.

At this time, the NGNP and LWRS project irradiation test requirements are more detailed than other DOE-NE programs. However, both projects rely heavily on PIE rather than real-time data obtained during irradiation testing. Efforts underway by the NEET, ATR NSUF, and FCRD programs are designed to develop and deploy in-pile sensors that can provide the required data during irradiation testing and assess the accuracy of data obtained with PIE to reflect conditions that occur during the irradiation.

2.4. Instrumentation Desired for DOE-NE Irradiations

As indicated in Section 2.3, it is anticipated that irradiation testing of fuels or materials will be performed by many DOE-NE programs. As discussed in Reference 30, sensors that are currently available at other MTRs (see Table 2-3) can be used to obtain many of the desired parameters with the accuracies specified in Tables 2-1 and 2-2. However, many of the sensors used at other MTRs need enhancements before they can be successfully deployed in the higher flux, harsher test conditions typical of ATR and HFIR tests. Many DOE-NE programs are funding efforts to enhance these sensors such that they can withstand anticipated ATR and HFIR test conditions required by DOE-NE research. As each enhancement activity is completed, new sensors are available to measure parameters, such as temperature, thermal conductivity, and creep elongation. However, in general, the resolution available with such sensors is limited due to the limited size of the irradiation test and the desire to minimize the impact of the sensor on test results. It should also be noted that existing and near-term sensor technology development efforts will not provide any capability for detecting changes in fuel microstructure or constituent migration.

Within the FCRD program, a workshop was held in November 2010 to identify candidate advanced technologies that could provide additional parameters with enhanced resolution and accuracy that are not currently measured during fuel irradiations.[1] During the workshop, international experts from industry, academia, and research organizations discussed possible criteria and agreed to rank candidate technologies using the following five items:

- *Potential to detect parameters with desired accuracy.* A noted objective of the FCRD effort is to develop instrumentation capable of unprecedented accuracy and resolution for obtaining the data needed to characterize three-dimensional changes in fuel microstructure during irradiation testing. Many of the candidate technologies offer the potential for improved detection of the ‘higher priority’ parameters (e.g., thermal properties, cracking, porosity, etc.) identified by fuel modeling experts. However, experts agreed that there were limited sensor technologies offering the potential to directly detect changes in fuel microstructure during irradiation testing, which is one of the highest priorities in the FCRD program.
- *Potential to detect desired parameters in prototypic conditions (environment, temperature, etc.).* Although experts recognized that some tests could be performed in non-prototypic conditions (e.g., metallic fuel surrounded by inert gas), it was agreed that such tests must be carefully planned to demonstrate their applicability. Hence, sensors that have the potential to provide data in prototypic conditions were ranked more highly.
- *Versatility.* Reference 1 identifies several parameters desired by fuel modeling experts. However, the size of irradiation tests limits the number of sensors that can be installed in a single test. Hence, experts viewed a single probe that can be used to detect a parameter at multiple locations more favorably. Likewise, from a funding perspective, a single technology that can provide data for detecting multiple parameters was ranked more highly because it offers the FCRD effort more opportunities.
- *Ease of Installation.* Instrumented test rigs are complicated. The ease with which a sensor can be installed is another important consideration. Clearly, sensors are more desirable (and ranked more

Table 2-3. Summary of sensors deployed at MTRs.

Parameter	Sensor	Operating Conditions	Accuracy
Temperature	Melt Wires	100-1200 °C	2-3 °C, but limited by number of wires with different melting points included in test.
	SiC monitors	100-800 °C	2%
	Thermocouples (N, K)	100-1000 °C	2%
	Thermocouples (High Temperature Irradiation Resistant Thermocouples (HTIR-TCs)	100-1800 °C	2%
	Thermocouples - Type C, D, R, and S	100-2000 °C	2% or worse, decalibrate due to transmutation
	Ultrasonic Thermometers[a]	1300 - 3000 °C	2%
Thermal Conductivity	Multiple Thermocouple	100-2000 °C, depending on thermocouple type	2-8%
	Hot Wire Needle Probe	100-2000 °C, depending on materials selected	2%
Density / Geometry Changes	Length - Linear Variable Differential Transformers (LVDTs)	up to 500 °C[b]	1-10 μm
	Diameter - Diameter Gauge	up to 500 °C[b]	1-10 μm
Crack Initiation /Growth	Crack Length - Direct Current Potential Drop (DCPD) Method	350 °C/2250 psia	~20%
Young's Modulus	Loaded Creep Specimen	up to 500 °C[b]	~10%
Fission Gas/Pressure	Sampling	Numerous isotopes	Unknown
	Pressure gauge	15 bar (220 psi) to 70 bar (1020 psi)	±0.2 bar (2.9 psi) to ±0.5 bar (7.3 psi)
Flux - Thermal	Flux wires / Foils	Material dependent	~10%
	SPNDs	Dependent on emitter	~1-10%[c]
	Fission Chambers	Dependent on fissile deposit	~1-10%[c]
Flux - Fast	Flux wires / Foils	Material dependent	~1-10%
	Fission Chambers	Dependent on fissile deposit	~1-10%

a. Prior in-pile use typically limited to short duration, fuel damage tests.
b. Some loss of accuracy at 350 °C due to Curie temperature effects, unless developmental LVDTs are deployed.
c. Accuracy decreases with use.

highly) if they can be installed without concerns about bends, breakage, special connectors, or a line of sight.

- *Technology Readiness (demonstrated in-pile experience to obtained desired accuracy under desired conditions).* Funding resources for the FCRD instrumentation development effort are limited. Technologies are less desirable if they require large investments to overcome large technology hurdles prior to deployment. Although experts deemed that all of the technologies described would require some investment to assess their viability for in-pile testing, experts favored technologies that could be deployed with less investment.

Results indicate that experts favored more mature technologies. Specifically, experts emphasized that existing research demonstrates that ultrasonic technologies offered the potential for some quick successes. For example, prior use of ultrasonic thermometers suggest that a single probe could be used to obtain a temperature profile with accuracies and resolutions not possible with existing technologies.

Experts also favored technologies that could obtain the desired data under prototypic conditions and if they offered the potential to detect most, if not all, of the parameters requested by fuel modeling experts. For example, ultrasonic sensors were ranked higher because of their potential to detect desired parameters in metallic fuel surrounded by sodium and in oxide fuel surrounded by helium for the range of temperatures of interest.

Experts also ranked technologies more highly if they offered the potential for 'diverse' parameter detection. For example, initial research investments in ultrasonic technologies could lead to methods that could ultimately be used to detect a wide range of parameters (e.g., physical and environmental parameters). Based on results from this workshop, efforts to develop one ultrasonic sensor, an ultrasonic thermometer, was initiated by the FCRD program.

Nevertheless, several key obstacles were identified by the experts at this workshop that must be overcome prior to wide-range deployment of ultrasonics-based instrumentation for irradiation testing. Specifically, it was observed that additional irradiation testing was needed to assess the survivability of ultrasonics transducers and that enhancements were needed with respect to signal processing software to improve the accuracy and ease of use for in-pile applications of ultrasonics technologies. The NEET tasks described in this report document initial results to address these needs. Section 3 summarizes the ultrasonic transducer material irradiation test; including a description of the irradiation test conditions, a discussion of the transducer materials and sensors included in the test, a description of the test capsule, and test results to date. Section 4 summarizes work toward the enhanced signal processing capabilities needed for future development of in-pile ultrasound based sensor systems and documents the evaluation of a signal processing algorithm used with prototypic ultrasonic thermometry data.

3. TASK 1: ULTRASONIC TRANSDUCER IRRADIATION TEST

There is a need to characterize and track the degradation during irradiation of candidate new fuels and structural materials. Such improvements will focus on refined temperature, displacement, and microstructure evolution measurements using advanced techniques and materials. As discussed in Section 2.2, real-time, high accuracy, data obtained from ultrasound-based sensors offer unique capabilities to better address this need.

Ultrasonic measurements have a long and successful history of use for out-of-core materials characterization applications, including detection and characterization of degradation and damage.[31] PIEs have successfully shown that fuel microstructural parameters, such as porosity and grain size, can be correlated to acoustic velocity.[32] According to Villard,[33] frequency requirements for such measurements are restricted to greater than 10 MHz. However, lower frequencies can be used for some applications, such as ultrasonic thermometry, where frequency requirements may be 100 – 150 kHz or lower.[34]

The development of ultrasonic tools to perform a variety of in-pile measurements requires a fundamental understanding of the behavior of ultrasonic transducer materials in high-radiation environments. While a number of irradiation studies of ultrasonic transducers have been described in the literature, a one-to-one comparison of these studies is difficult, as the materials and irradiation test conditions often differ. In addition, the tests to date are generally at lower flux/fluences than what might be seen in US MTRs. As a result, a series of experiments to baseline the performance of ultrasonic transducer materials (in terms of change in sensitivity as a function of temperature and irradiation) are necessary to support the irradiation test.

Task 1 of this project leverages ATR-NSUF funded efforts to develop a test capsule design and define irradiation conditions for evaluating the most promising candidate piezoelectric and magnetostrictive transducer materials and designs. From the onset of this effort, an instrumented lead test was proposed, such that real time signals are received from the transducers being tested. Collecting real time signals enables an accurate measure of the performance and possible degradation of candidate transducer and sensor materials under irradiation. The objective for Task 1 of this project is to evaluate the performance of ultrasonic transducer materials in high flux/high temperature irradiation environments.

Results of this irradiation test provide important data on irradiation performance to assist in the development and deployment of ultrasonic sensors for in-pile measurements, including fuel and material morphology changes, fission gas composition and pressure measurements, fuel and material geometry changes, and temperature. In addition, radiation test results provide a technical basis for selecting optimum (with respect to in-core survivability) ultrasonic transducer materials for different in-pile measurements and guide the development of signal processing tools to enhance the measurement to demonstrate the intended in-pile measurements.

The PSU-led proposal for an ultrasonic transducer irradiation was selected by the ATR NSUF for irradiation in the MITR. A flowchart describing the responsibilities of each collaborating organization and the scheduling for completing the activities associated with Task 1 is shown in Figure 3-1. It should be noted that MIT was funded by the ATR NSUF and that the industry partner and CEA participated at their own expense. This section documents results from this effort. Additional details of work completed in this project are documented in the FY-12 and FY-13 status reports.[13, 14] Data (up to the time that this report was prepared) from transducers and instrumentation included in this test are presented. It should be noted that this ATR NSUF irradiation will extend beyond the duration of this NEET project. Remaining data from instrumentation in this irradiation and results from planned PIEs will be documented using ATR NSUF funding.

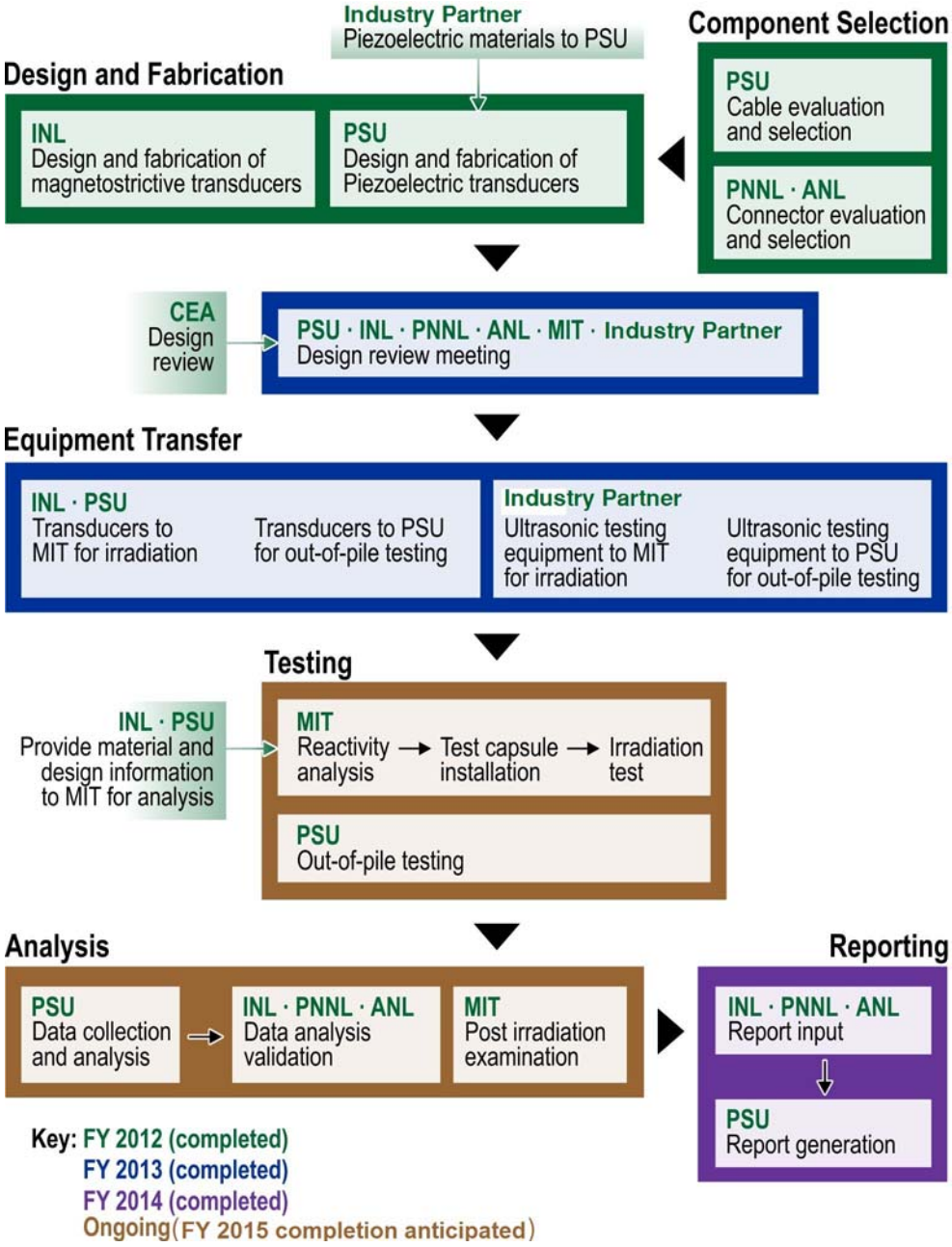

Figure 3-1. Task 1 schedule flow chart (Colors reflect years in which tasks were initiated; estimated end date is shown in parenthesis).

3.1. Test Capsule Design

3.1.1. MITR Design

As noted above, the ultrasonics transducer irradiation is being performed in the MITR. Relevant MITR design information is summarized here to provide perspective about the design of the ultrasonics transducer capsule and test conditions developed by this project.

The MITR is a tank-type research reactor.[35] It is currently licensed for 6 MW operation. The identified irradiation position and associated flux conditions at this location in the MITR are summarized in Table 3-1.

Table 3-1. Representative dimensions and flux levels in MITR.

MITR In-Core Experimental Facility
Irradiation tube for sample capsule irradiation or isotope production (instrumented or uninstrumented.)
Coolant loops that replicate conditions in either pressurized and boiling water reactors.
Facilities for testing mechanical properties of samples in a light water reactor environment.
High temperature irradiation facility for materials irradiations in inert gas (He/Ne mix) at temperatures up to 1400 ^{o}C.
Size: Space for 3 capsules Max in-core volume ~ 46 mm ID x 610 mm long
Neutron Flux (n/cm^2-s): Thermal: ~3.6 x10^{13} Fast: up to 1.2x10^{14} (Energy>0.1 MeV)

The ATR-NSUF/PSU test capsule is limited to a 46 mm diameter and a 610 mm length. Temperature control is afforded by a helium/neon gas gap with adjustable gas composition. The test temperature at full reactor power has been approximately 400-450 ^{o}C. In order to observe rapid changes at relatively low fluences, the test was started with the reactor slowly coming to power over approximately 150 hours. The steady state fast flux (Energy>1 MeV) is 3.5x10^{13} with reactor running at 5.8 MW power. This level of fast flux requires approximately 390 full power days, or 23 calender months, to reach the desired fluence level of at least 1x10^{21} n/cm^2 (Energy>1.0 MeV).

Figure 3-2 shows the position of the test capsule within the MITR core. Based on thermal analysis performed at MIT, the expected operating temperature for the test at steady state was estimated to range between 350 and 450 °C. This initial analysis has proven accurate. After startup, the target temperature has been controlled by variation of the composition of a gas gap between the test capsule and the in-pile experiment tube. The gas is a mixture of helium and neon.

As discussed in this section, this irradiation is the first to evaluate and characterize such a wide range of transducer materials to such high fluences, with diverse instrumentation to fully characterize the irradiation conditions. The capsule was inserted into the MITR on February 18, 2014; and a gradual power ramp was started on February 19, 2014.

3.1.2. Capsule Design

Details of the preliminary capsule design are available in the FY-12 and FY-13 status reports.[13, 14] The final design accommodates four piezoelectric transducers and two magnetostrictive transducers. All of the originally selected transducer materials were included, but only the AlN transducer has a redundant transducer. A key feature of the redesigned capsule is the staggering of the vertical position of each piezoelectric transducer. This feature spreads the mass of the transducers across a greater volume and reduces the concentrated gamma heating. All of the originally proposed instrumentation has also been included, as have stand-alone samples of each candidate transducer material. The final design is shown in Figure 3-3.

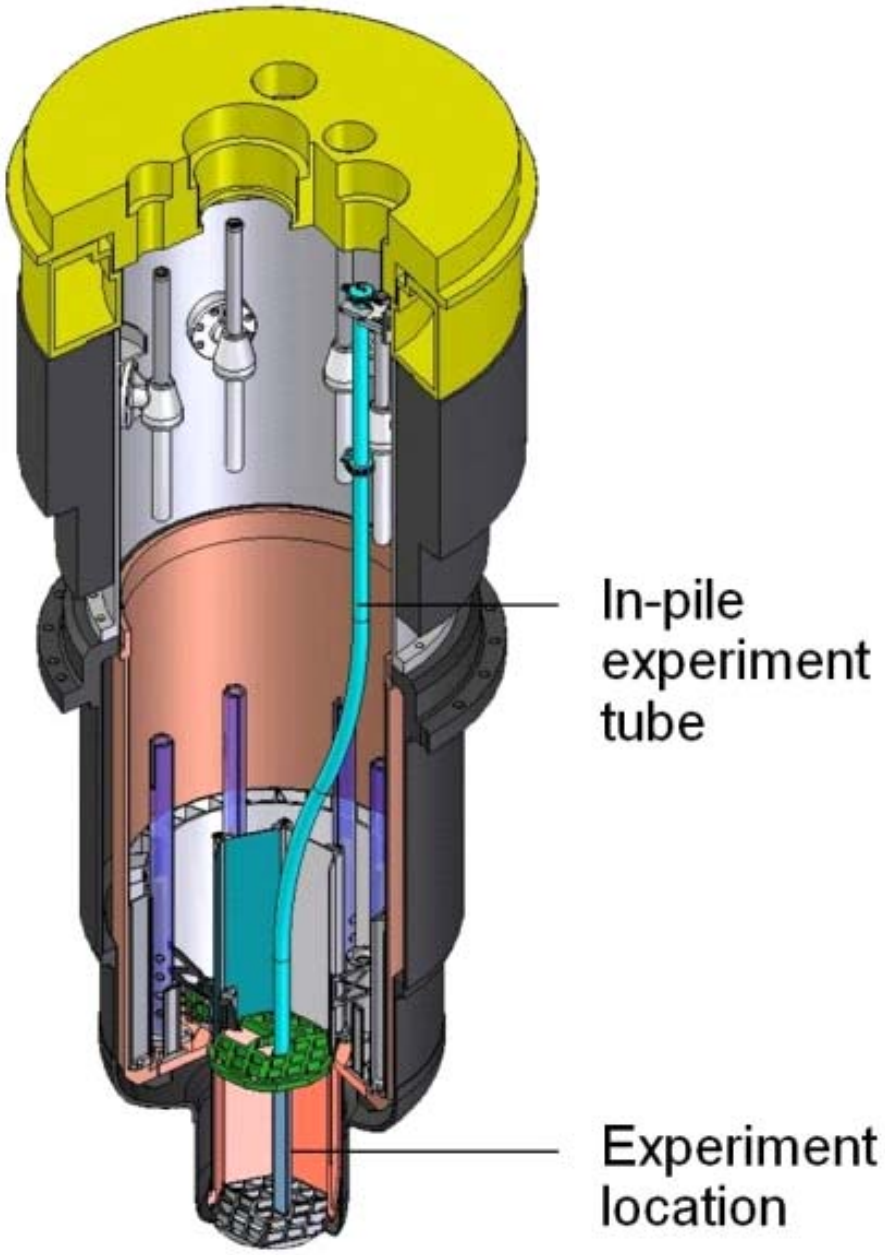

Figure 3-2. Position of irradiation capsule within MITR core.

3.1.3. Sensors

In order to characterize ultrasonic transducer degradation during irradiation, real-time data are needed on the irradiation test conditions. As discussed within this section, the test includes diverse and redundant instrumentation for monitoring irradiation test conditions.

Irradiation test temperatures is monitored online by two Type-K thermocouples with junctions located at different axial positions. Thermal neutron flux is monitored online by a vanadium emitter Self Powered Neutron Detector (SPND). Gamma flux is monitored online by a platinum emitter Self Powered Gamma Detector (SPGD). A schematic diagram of the SPND and SPGD is shown in Figure 3-4 [Sensors have identical configuration and dimensions, selected sheath materials (Inconel 600), and insulation material

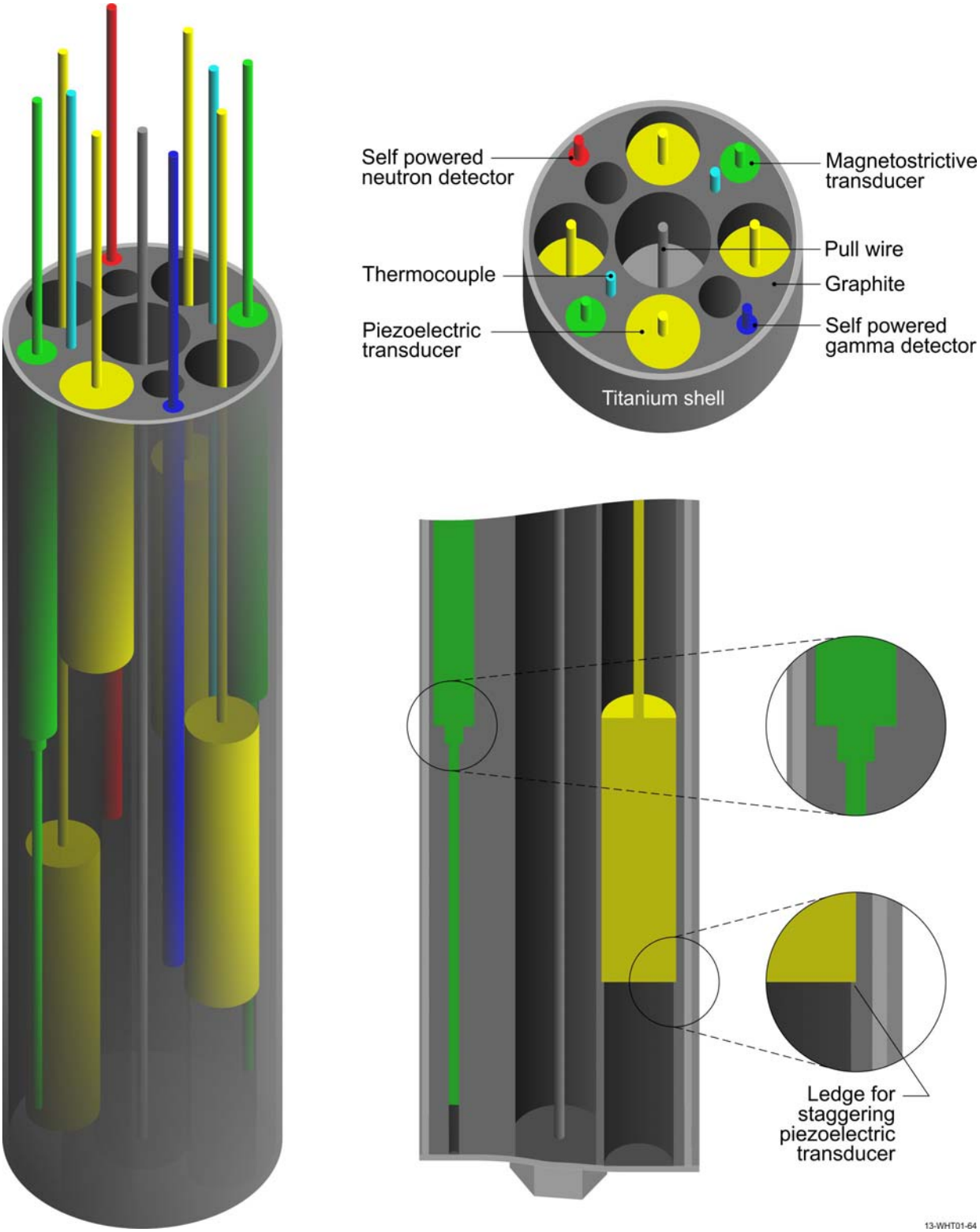

Figure 3-3. Final test capsule graphite sample holder design with sample and instrumentation positions detailed.

(Al_2O_3). Differences are limited to the selected emitter (e.g., vanadium for the SPND and platinum for the SPGD)].

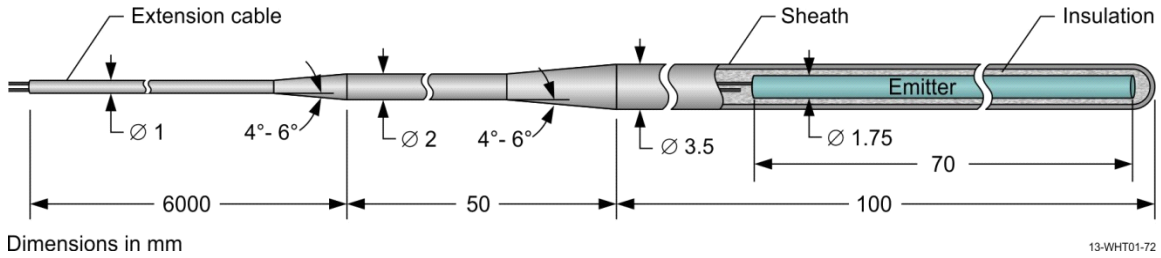

Figure 3-4. Schematic diagram of SPND and SPGD (dimensions are the same for each).

In addition to the thermocouples, the maximum temperature reached at selected locations during the irradiation will be verified during post irradiation examination using melt wires encapsulated in a quartz tube. Five wire compositions have been included, with melting temperature ranging between approximately 327 ^{o}C and 514 ^{o}C. Melting temperatures of the wires were verified by High Temperature Test Laboratory (HTTL) staff using a Differential Scanning Calorimeter (DSC). Melt wire compositions and melting temperatures are listed in Table 3-2, and a photo of a quartz-encapsulated melt wire capsule is shown in Figure 3-5. Integrated thermal and fast neutron fluences at selected locations will be evaluated through post irradiation analysis of Fe-Ni-Cr flux wires.

Table 3-2. Compositions and melting temperatures of melt wires.

Material Composition, %	Melting Temperature, ^{o}C
100 Pb	327.5
94 Zn-6 Al	381.0
85 Te-15 Sn	401.0
100 Zn	419.6
80 Sb-20 Zn	507.8-514.3

Figure 3-5. Example melt wire capsule with four wire types.

3.2. Transducers

To generate and receive ultrasonic pulses and signals, the two most commonly used methods rely on piezoelectric or magnetostrictive materials. Ultrasonic measurements using piezoelectric transducers have been demonstrated over a wide frequency range from kHz and up to GHz; however, most non-destructive examination (NDE), materials characterization, and process monitoring are performed in the range from 1-20 MHz, making piezoelectric transduction ideal. The current capabilities of magnetostrictive transducers are typically limited to operation at frequencies up to the order of 100 kHz, though recent research suggests that higher frequencies may be possible for small transducers. However, mechanical coupling, as well as enhanced guided wave mode generation, makes magnetostrictive transduction ideal for low frequency measurements, such as ultrasonic thermometry.[36] Therefore, radiation tolerant sensors which uti-

lize piezoelectric or magnetostrictive materials are being considered as candidates for instrumentation and US MTR testing.

Prior studies have shown that typical piezoelectric and magnetostrictive materials used in transducers degrade when subjected to high temperature and radiation.[37-42] Candidate magnetostrictive and piezoelectric materials must, therefore, be carefully selected; and transducer assemblies must be carefully designed. As discussed below, only limited radiation effects data are available to guide this process.

The MITR irradiation test and associated laboratory evaluations (to be performed by PSU in FY-15) supported by this project will provide important information for selecting appropriate transducers for ultrasonic sensors.

INL and PSU developed and fabricated transducer designs for the MITR irradiation. As reported in this subsection, both piezoelectric and magnetostrictive transducer designs were developed, successfully fabricated, and shipped to MIT.

3.2.1. Piezoelectric Materials

A literature review was completed at the beginning of this effort to identify candidate piezoelectric transducer materials. The piezoelectric materials selected for inclusion in the irradiation test are summarized in Table 3-3. Additional details related to candidate piezoelectric transducer materials may be found in Reference 13.

Table 3-3. Candidate piezoelectric materials.

Material	Composition	Transition Temperature, °C	Transition Type	Comments
Bismuth Titanate	Bi_3TiO_9	909	Curie Temperature	Thought to be radiation tolerant. Most promising previously tested candidate. Good baseline comparator.
Aluminum Nitride	AlN	2200	Melt	Thought to be highly radiation tolerant. Very high temperature capability.
Zinc Oxide	ZnO	>1500	Melt	Thought to be highly radiation tolerant. High temperature capability.

Aluminum Nitride (AlN)

Aluminum nitride is a relatively new material, as far as bulk single crystals are concerned. In fact, the work of Parks & Tittmann[43] assessing this material is the first. In the past, thin film AlN was shown to be unaffected by gamma irradiation up to 18.7 MGy[44] and temperatures of 1000 °C.[45,46] Moreover, this material has been explicitly cited in numerous independent studies as a highly radiation tolerant ceramic.[47]

Further, tests of bulk single crystal AlN in a TRIGA nuclear reactor core showed this material to be completely unaffected by fast and thermal neutron fluences of 1.85×10^{18} n/cm^2 and 5.8×10^{18} n/cm^2, respectively, and a gamma dose of 26.8 MGy.[43] This work, along with that of Yano[48] and Ito,[49] have indicated that the $^{14}N(n,p)^{14}C$ reaction is not of much concern with respect to degradation.

Bismuth Titanate Niobate (Bi_3TiO_9)

The literature review has revealed bismuth titanate niobate to be the most promising previously tested material.[50] However, this material lost roughly 60% of its one way piezoelectric response at a fast neutron fluence of 10^{20} n/cm^2, which may preclude it from being used for longer duration in-pile irradiations. The decrease in the signal response is in agreement with the statements made by Trachenko,[47] namely that disordered Ti-O-Ti bridges of highly covalent character form in titanates when subjected to ballistic radiation

effects. Regardless, given that this material has shown the greatest promise to date of previously tested materials, it was selected as a baseline in this research effort.

Zinc Oxide (ZnO)

Zinc oxide is found in the Wurzite structure, as is AlN, and has been cited as a highly radiation tolerant material.[47] The evaluated nuclear data files (ENDF)[51] do not show any detrimental nuclear cross sections, and this material possesses a high transition temperature and moderate piezoelectric coupling.

3.2.2. Piezoelectric Transducer Design

The design of the piezoelectric transducers developed for this irradiation is based on the design used in a prior Training, Research, Isotopes, General Atomics (TRIGA) test of AlN.[43] The piezoelectric transducers use pressure for coupling the piezoelectric element to the stainless steel waveguide. Electrical contact with the piezoelectric element is also achieved through application of pressure. A backing layer behind the piezoelectric sensor provides damping (preventing excessive "ringing" of the transducer) and acts as an electrode. The electrical connection from the lead-in cable to the graphite backing is made through a stainless steel plunger, which is isolated from the housing by alumina insulation. The connection to ground is made through the housing, with the waveguide acting as the second electrode. Transducer performance is measured using pulse-echo measurements through the stainless steel waveguide. A schematic of the design is shown in Figure 3-6.

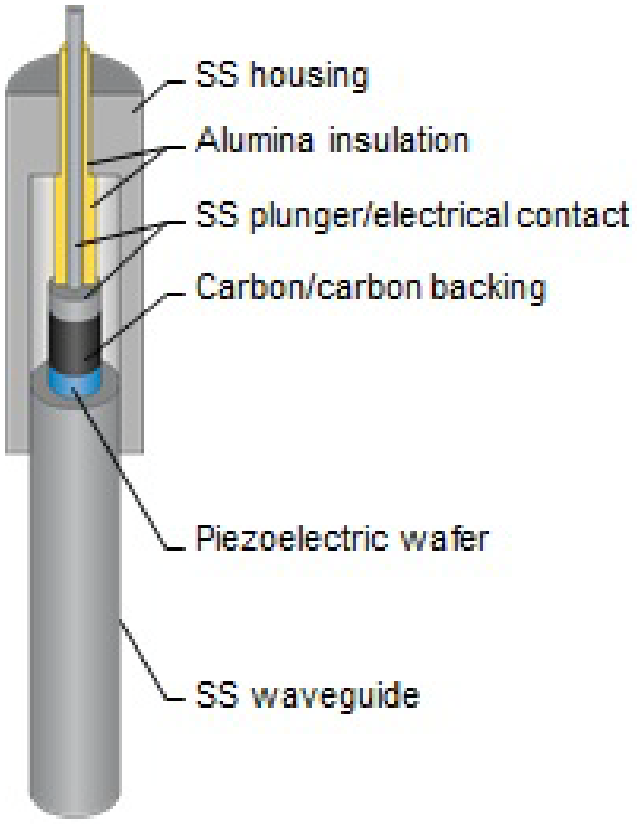

Figure 3-6. Piezoelectric transducer design.

Figure 3-7 shows a piezoelectric transducer prior to assembly. Figure 3-8 shows a close up view of a ZnO crystal in the as-received state.

Figure 3-7. Two piezoelectric transducers laid out prior to assembly.

Figure 3-8. ZnO piezoelectric crystal prior to incorporation into transducer.

Originally, a slip joint was made from an alumina insulation bead to mechanically hold the lead cable to the plunger. However, upon delivery of the samples to MIT, it was discovered that this method did not provide sufficient support. A picture of the original alumina sleeve design is shown in Figure 3-9(a). The sleeve is bonded to the wire sheath using a castable mineral cement while the lead wire is left exposed in the center of the sleeve. The plunger is fit into the sleeve making mechanical contact with the lead wire. To compensate for this, a strain relief fixture was designed to stabilize the connection. The transducer with the strain relief sleeve installed is show in Figure 3-9(b).

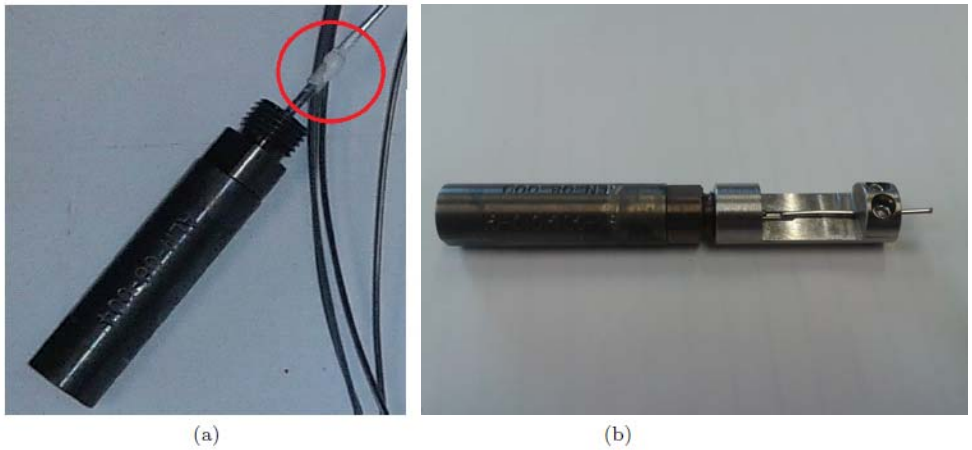

Figure 3-9. Piezoelectric transducers: (a) with alumina bead connection to extension cable, (b) with strain relief sleeve designed to support connection to cable.

3.2.3. Magnetostrictive Materials

A literature review was also completed at the beginning of this effort to identify candidate magnetostrictive transducer materials. Additional details related to candidate magnetostrictive transducer materials may be found in Reference 13. The magnetostrictive materials included in the irradiation test are summarized in Table 3-4.

Table 3-4. Candidate magnetostrictive materials.

Material	Composition	Key Properties	Comments
Remendur	49Fe-49Co-2Va	70-100 μ-strain max. magnetostriction, curie temperature 950 °C	No longer manufactured, identical/similar alloys available, possible activation of cobalt
Galfenol	Fe-14Ga-NbC	100-400 μ-strain max. magnetostriction, curie temperature 700 °C	Relatively new, small amounts of data, difficult to acquire
Arnokrome 4	95Fe-5Cr	10-40 μ-strain max. magnetostriction, curie temperature 770 °C	Low magnetostriction, included as loose sample
Arnokrome 5	92Fe-8Mn	10-40 μ-strain max. magnetostriction, curie temperature 770 °C	Low magnetostriction, included as loose sample

Remendur

Remendur has the most history of use in nuclear applications of all the magnetostrictive alloys, having been used previously for short duration thermometry applications.[52-55] Remendur has relatively high Curie temperature and magnetostriction. Although Remendur is no longer commercially available, several identical alloys are available under different names. INL has a supply of Remendur which was used for this test.

Galfenol[56]

Galfenol is a relatively new alloy of iron and gallium. Galfenol is a member of the “giant” magnetostrictive alloys and has a very large saturation magnetostriction. It also has an appropriately high Curie temperature. Neither constituent element reacts strongly with neutron radiation.

Arnokrome™ (Arnold Magnetics[57-59])

Arnold Magnetics produces several magnetostrictive alloys, Arnokrome 3, Arnokrome 4, and Arnokrome 5. Arnokrome 3 contains cobalt and has much lower magnetostriction than Remendur. Hence, it was omitted from in the current study. Arnokrome 4 and 5 have similar magnetostriction to Arnokrome 3, but without the presence of cobalt. The Arnokrome alloys appear less promising than the other selected materials and due to test capsule limitations were not included in the irradiation as a transducer material. However, samples of Arnokrome 4 and 5, along with all the other magnetostrictive and piezoelectric materials, were included in the irradiation test as stand alone samples (not incorporated into a transducer).

3.2.4. Magnetostrictive Transducer Design

The magnetostrictive design developed for this effort was influenced by prior research to develop an appropriate transducer for use in ultrasonic thermometry applications.[52-55] In particular, magnetostrictive transducer fabrication efforts were leveraged from FCRD-funded efforts to develop an ultrasonic thermometer. A schematic of the magnetostrictive transducer design is shown in Figure 3-10. Dimensions of the transducer housing pieces are shown in Figure 3-11. The original design planned for inclusion in this irradiation included a biasing magnet, a spring, and a damper. The biasing magnets were eliminated based on results from laboratory evaluations. It was determined that the spring (used to tension the waveguide

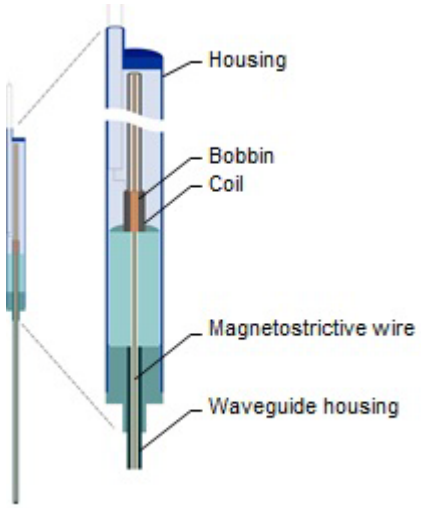

Figure 3-10. Magnetostrictive transducer design.

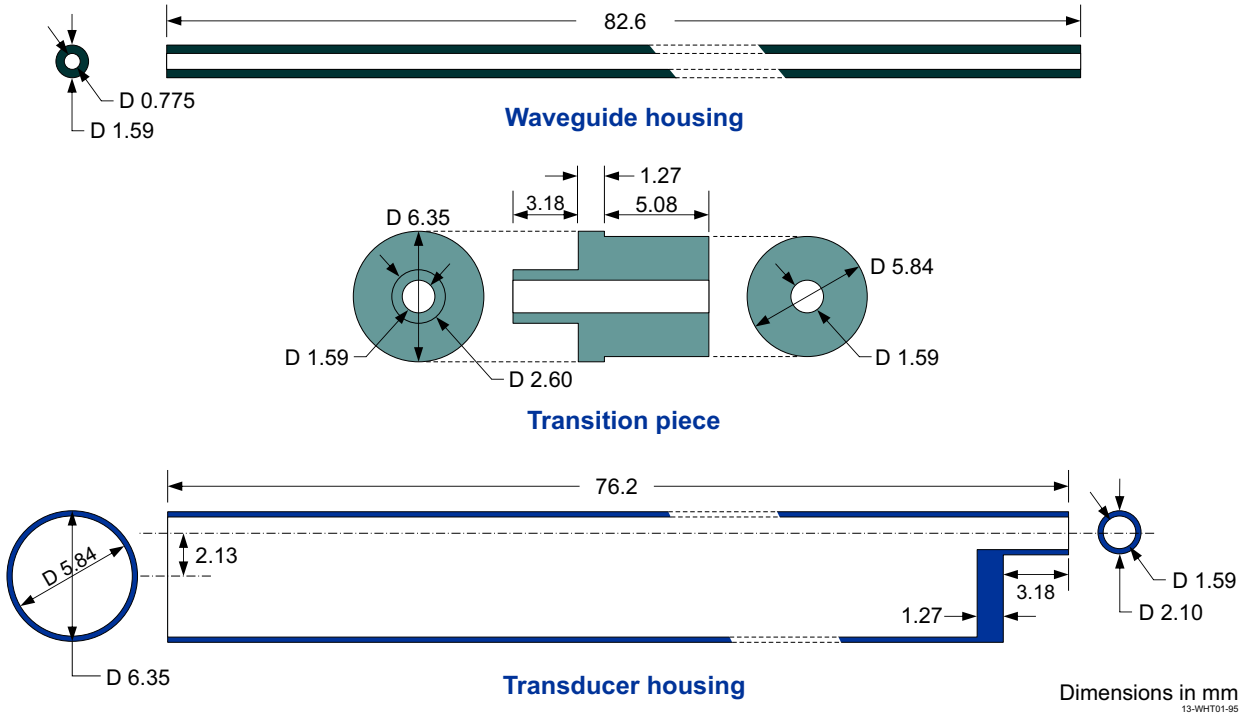

Figure 3-11. Transducer housing dimensions.

and reduce contact with the housing) and the damper (used to eliminate reverberations) were unnecessary and complicated the construction process. Incidental contact between the waveguide and housing can have an effect on the shape of the recorded signal. However, the transducer performance is judged based on changes in the signal over time, and its initial shape is not critical. The damper eliminates multiple pass through signals, which will be used to determine attenuation characteristics of the waveguide material.

Construction of high temperature magnetostrictive transducers is a multi-step process that involves several heat treatment steps. First, the coil is formed by wrapping several layers of silver-palladium wire around an

alumina bobbin [see Figure 3-12(a)]. The wire is coated in a standoff insulation (a particulate alumina silica mix with a burnable binder). The insulation requires a heat treatment step prior to high temperature use, and the wire becomes brittle after heating [see Figure 3-12(b)]. After heat treatment, the coil is coated with alumina cement and heat treated a second time (to cure the cement) [see Figure 3-12(c)]. The coil is next securely placed in a fixture, and the wire leads are laser welded to a high temperature capable coaxial cable (one lead to the center conductor and one to the sheath) [see Figure 3-12(d)]. As the welds are fragile, the end of the cable and the coil are coated in another layer of alumina cement and cured. The magnetostrictive wire (previously welded to the waveguide) is then threaded through the coil. Last, the assembly is placed into a pre-fabricated transducer housing and seal welded [see Figure 3-12(e)].

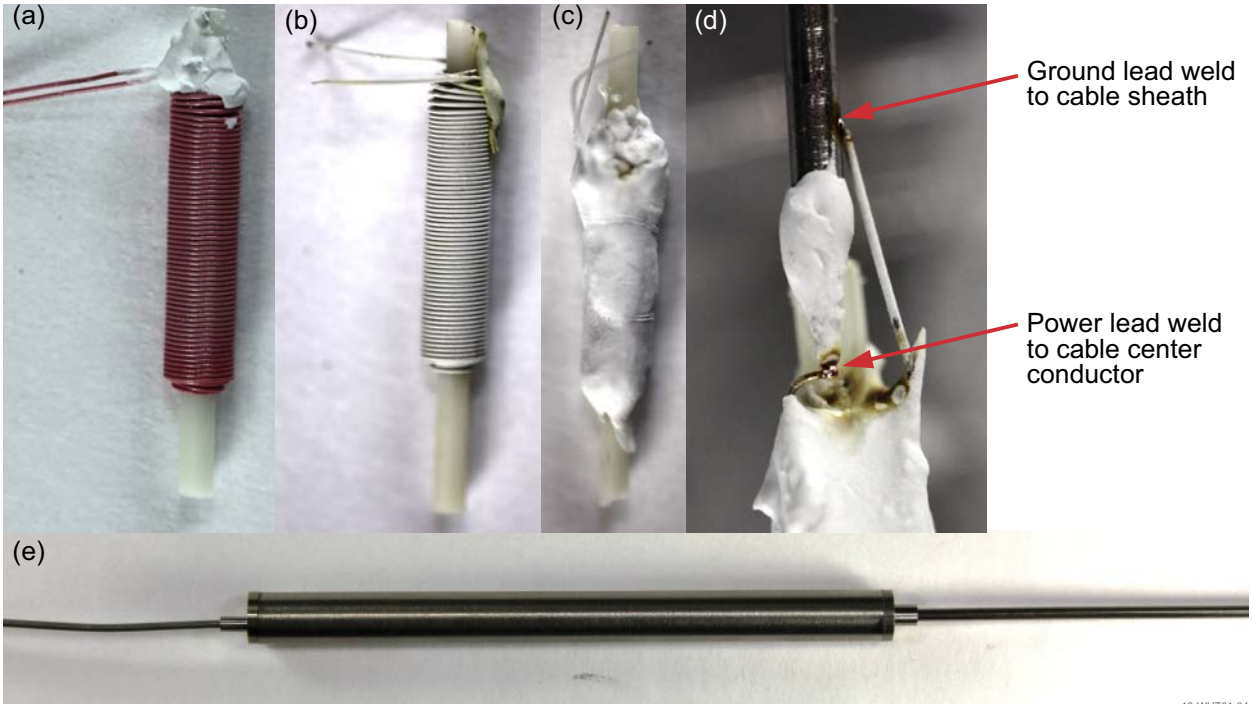

Figure 3-12. Steps involved in making high temperature capable magnetostrictive transducer.

3.3. Cables and Connectors

During FY13, efforts were made to finalize the requirements and procure cabling and connectors for this irradiation test. For each transducer or sensor in the MITR irradiation, there are three cables. The first cable connects the transducer (or sensor) to the MIT terminal box within the reactor vessel. This cable is denoted as Cable 1 (see Figure 3-13, note that only one of each cable is shown; there are actually 10 cables: six for the transducers, and four for the sensors). This cable is integral and was supplied, installed, with each transducer or sensor. The second cable extends from the terminal box to another terminal box just outside the reactor. This cable is denoted Cable 2 in the figure. The third cable extends from the junction box outside the reactor to the electronics cabinet.

Because there is a fairly large number of cables and because the cables must be flexible enough to be routed through relatively tight and tortuous quarters, the cables must be of small diameter as shown in Figure 3-14 and Table 3-5.

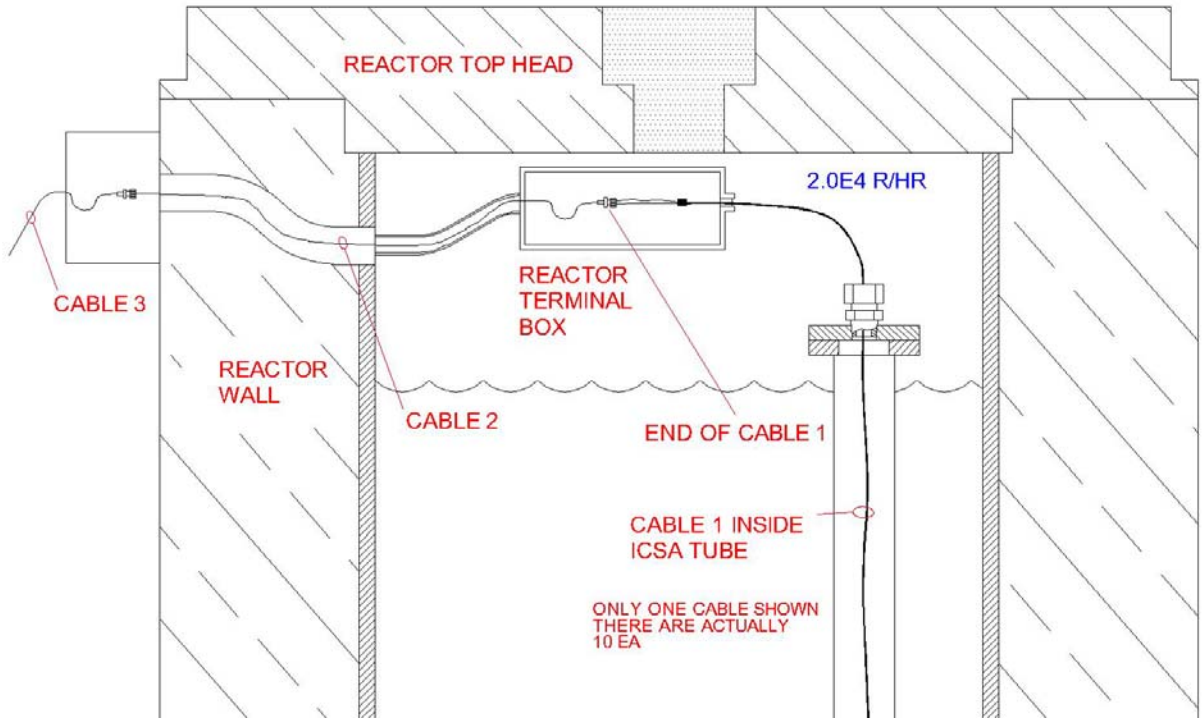

Figure 3-13. Cable details near reactor head.

Table 3-5. Characteristics of transducer extension cables.

	Cable 1	Cable 2	Cable 3
Length	6 m	<3 m	<16 m
Type	Co-axial, 50-ohm impedance, mineral insulated, metallic sheath, 1.0 mm OD.	Commercially available mini co-ax, 50 ohm impedance, RG-174.	Commercially available mini co-ax, 50 ohm impedance, RG-174.
Connectors	Connection to the transducers are mechanical connections. Connector at far end is BNC	Both connectors are BNC.	Both connectors are BNC.
Temperature	At transducer connection up to 450°C, elsewhere <70°C	<70°C for first few feet inside reactor, <40°C outside reactor	<40°C
Radiation Field	Up to 1E9 R/hr at connection to transducers diminishing to 2E4 R/hr at top of vessel	2E4 R/hr for first few feet inside reactor, negligible outside reactor wall	Negligible

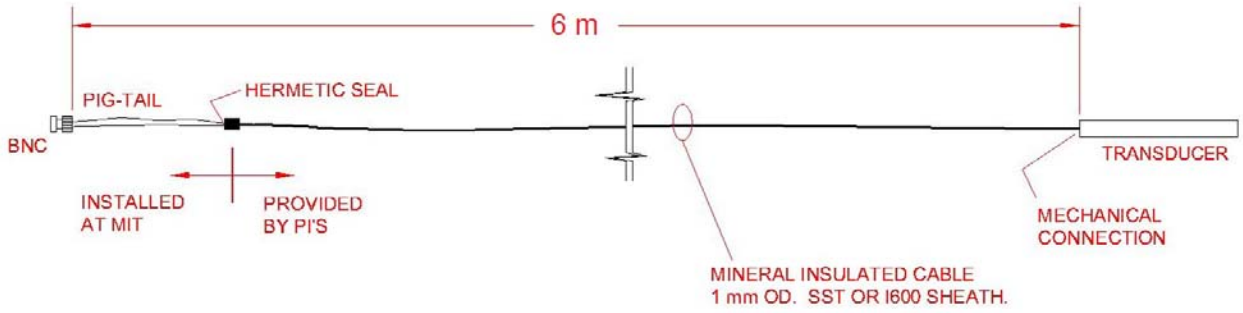

Figure 3-14. Detailed view of transducer cable 1-from transducer to junction box.

3.4. Irradiation Test Results to Date

The irradiation test started in late February 2014 and will run until either the target fast fluence (at least $1.0*10^{21}$ n/cm^2, >1 MeV) is reached or all test transducers have failed. As of September, 2014, a total fluence of approximately $4.1*10^{20}$ n/cm^2 has been reached. Signal changes, which are due to both radiation and temperature effects, are difficult to separate analytically. As such, only changes occurring while the reactor is operated at steady state (i.e. constant temperature) can be considered. Figure 3-15 shows the power and temperature history of the test to date. Differences in temperatures are due to different axial

position of the thermocouples within the test capsule. As noted previously, it is anticipated that the irradiation will extend beyond the duration of this NEET project. The remaining data from this irradiation and results from PIEs will be documented using ATR NSUF funding.

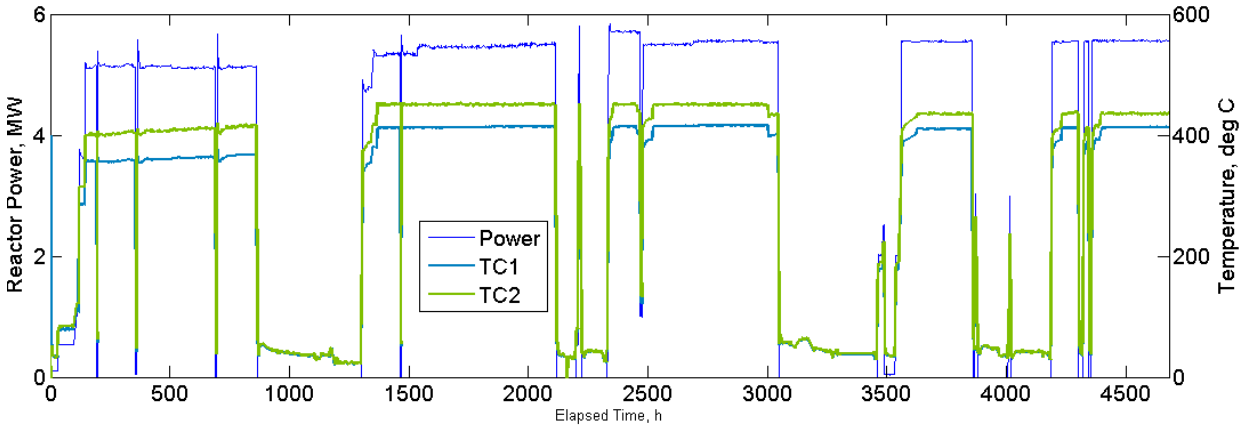

Figure 3-15. Reactor power and temperature history for ULTRA test.

3.4.1. Piezoelectric Transducer Performance

Two of the piezoelectric test transducers (the zinc oxide transducer and one of the aluminum nitride transducers) failed due to electrical connection issues during or just after reactor startup (see Figure 3-16). Hence, real time data for these transducers was not available for analysis. The materials will be evaluated during PIE, but this may not reveal useful information if the transducer materials have degraded significantly during irradiation.

The bismuth titanate performance was characterized by measuring the change, with respect to accumulated fluence, of the normalized magnitude of the first resonant frequency of the Fourier transform of the recorded A-scan (signal amplitude as a function of time) signal. The signal was observed to decease steadily during the early reactor cycles, up to a fast fluence of approximately $5.0*10^{19}$ n/cm^2. After this point, the transducer has shown a slow recovery, with sharp increases in amplitude during shutdowns, as seen in Figure 3-17. The cause of this behavior is unclear, but may be a result of changes to the coupling between the piezoelectric element and the metallic waveguide. PIE may reveal more about whether this is a function of mechanical changes to the transducer or changes in the crystal itself.

The performance of the aluminum nitride transducer was characterized by measuring the change, with respect to accumulated fluence, of the normalized magnitude of the resonant frequency of the Fast Fourier Transform (FFT) of the first waveguide reflection observed in the recorded A-scan signal. The aluminum nitride response has been stable, with the exception of rapid drops in signal strength accompanying rapid changes in the reactor condition (i.e., rapid flux and temperature changes), as shown in Figure 3-18. As with the bismuth titanate transducer, these rapid changes are likely due to sharp changes in coupling efficiency caused by the temperature changes. To this point in the irradiation, aluminum nitride appears to be a viable candidate for in-core use.

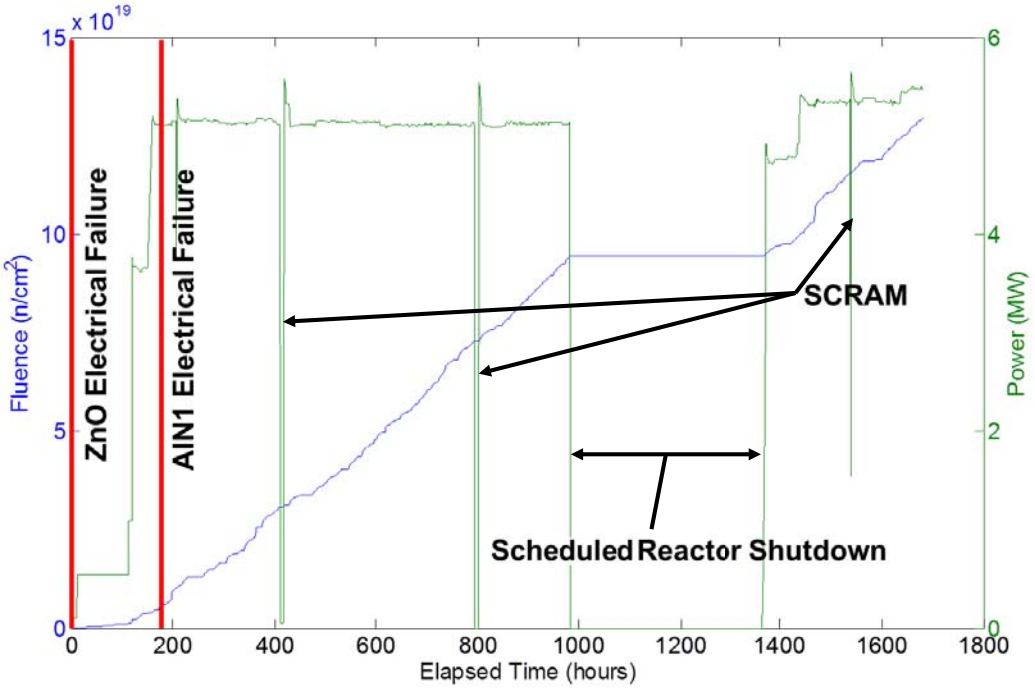

Figure 3-16. Early failure time of two piezoelectric transducers.

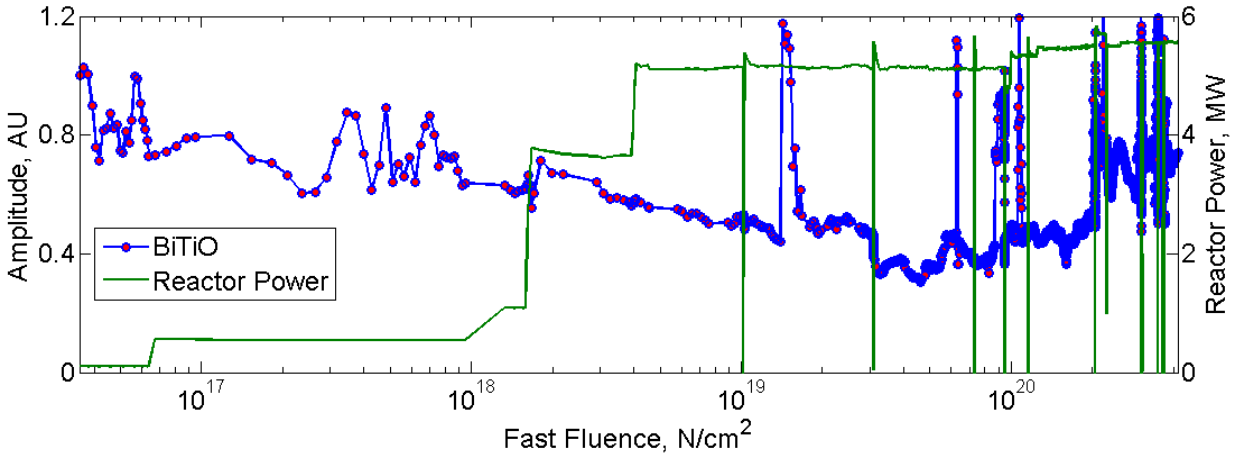

Figure 3-17. Bismuth titanate performance as a function of accumulated fast fluence.

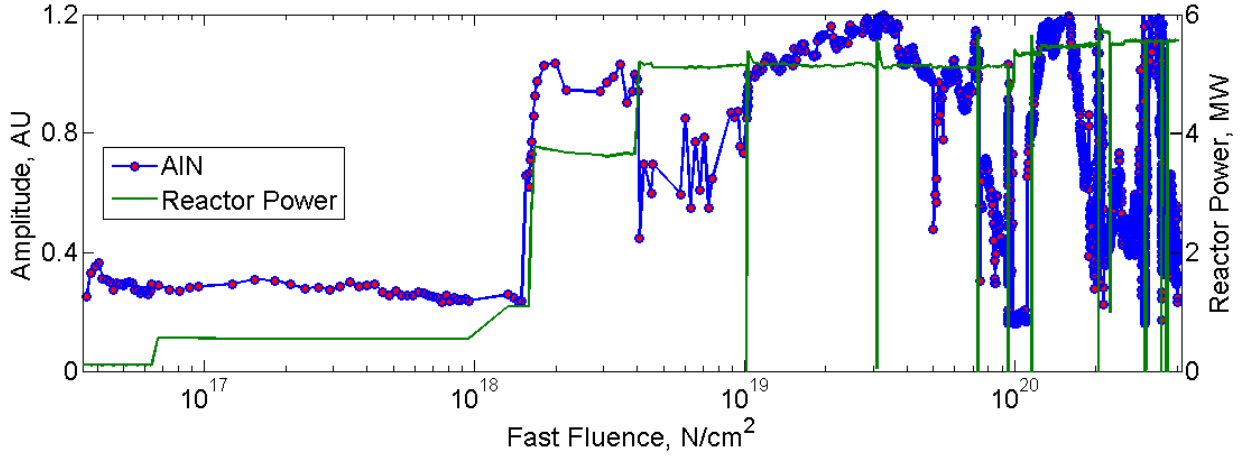

Figure 3-18. Aluminum nitride performance as a function of accumulated fast fluence.

3.4.2. Magnetostrictive Transducer Performance

Performance of the transducers is characterized using the same method as was used for the aluminum nitride transducer. The normalized magnitude of the FFT of the first waveguide reflection signal was used to track the change in signal strength (normalized to the signal when the reactor reached full power). The frequency transformed signal is used because it is less sensitive to the interference effects of noise and signal transients. The same method was used for the Galfenol transducer.

Figure 3-19 shows the normalized amplitude for the Remendur transducer as a function of accumulated fluence. The green trace corresponds to the reactor power history. Increased noise after the reactor was restarted after refueling may indicate an intermittent short in the drive coil. There is a general decreasing trend, but signal recovery after temperature transients indicate that some of the signal attenuation is due to temperature effects, in this case binding of the wire against the coil bobbin (see Figure 3-10 for transducer component diagram).

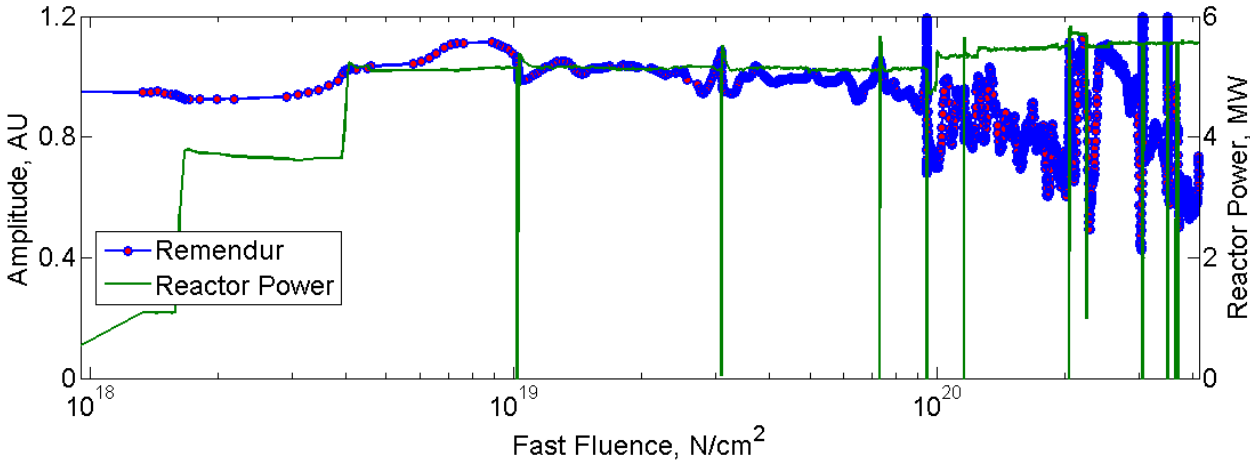

Figure 3-19. Remendur performance as a function of accumulated fast fluence.

The Galfenol transducer has shown very stable operation over the course of the irradiation, though the total peak to peak signal amplitude is typically on the order of one third of that observed for Remendur. Figure 3-20 shows the normalized peak to peak amplitude for the Galfenol transducer as a function of accumulated fluence. The green trace shows the reactor power history. The Galfenol transducer shows steady operation during periods when the reactor power level was stable. There is little decrease in the signal strength over these periods. The decreases in signal strength observed when reactor power is increased appear to be due to increases in operating temperature, as the signal strength stabilizes shortly after each power increase. As with the Remendur transducer, increased noise after the first reactor restart after refueling may indicate an intermittent short in the drive coil.

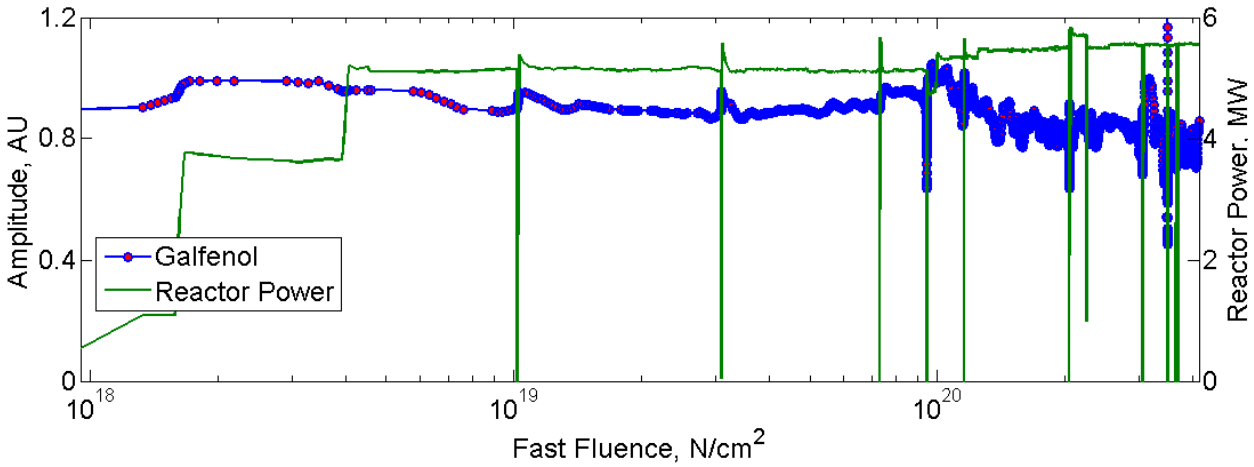

Figure 3-20. Galfenol performance as a function of accumulated fast fluence.

3.4.3. Self Powered Detector Performance

Figure 3-21 shows data obtained from the SPND and SPGD sensors included in this irradiation. Although trends in the SPND and SPGD signals have generally been in agreement with trends in the reactor power, some discrepancies have been observed. First, during the slow, stepwise initial reactor startup, the SPGD signal was observed to overshoot (relative to the reactor power signal) and then slowly recover; this is shown in Figure 3-22, which shows the last stepwise power increase during startup. Although a satisfactory explanation is not available, conversations with CEA collaborators (who have observed similar behavior) indicate that this behavior occurs only during the initial start up and will have no further impact on the reported data. Possible explanations include thermal annealing and electronic rearrangement under irradiation.

A separate effect, which appears to be temperature dependant, has also been observed. Figure 3-23 compares signals from the SPND and SPGD with the Type K thermocouple located in the lower section of the test capsule. This thermocouple is used for test temperature control. At several points during the irradiation, the temperature was varied slightly while reactor power was held constant. This was accomplished by varying the gas composition (thereby varying the thermal conductivity) in the experiment tube. The effect appears as a change in detector sensitivity that is inversely proportional to a sudden change in temperature, followed by a slow recovery.

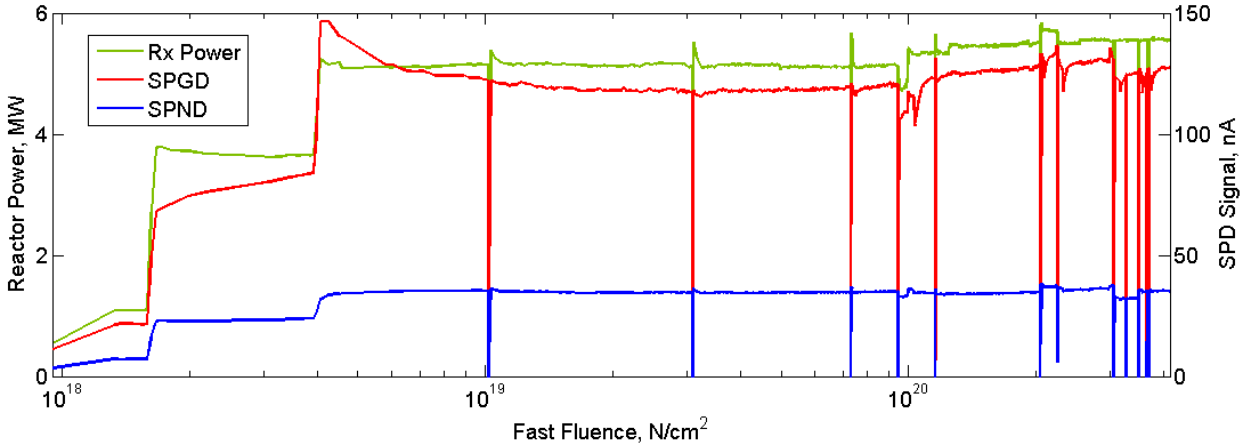

Figure 3-21. Self powered detector signals and reactor power as a function of fluence.

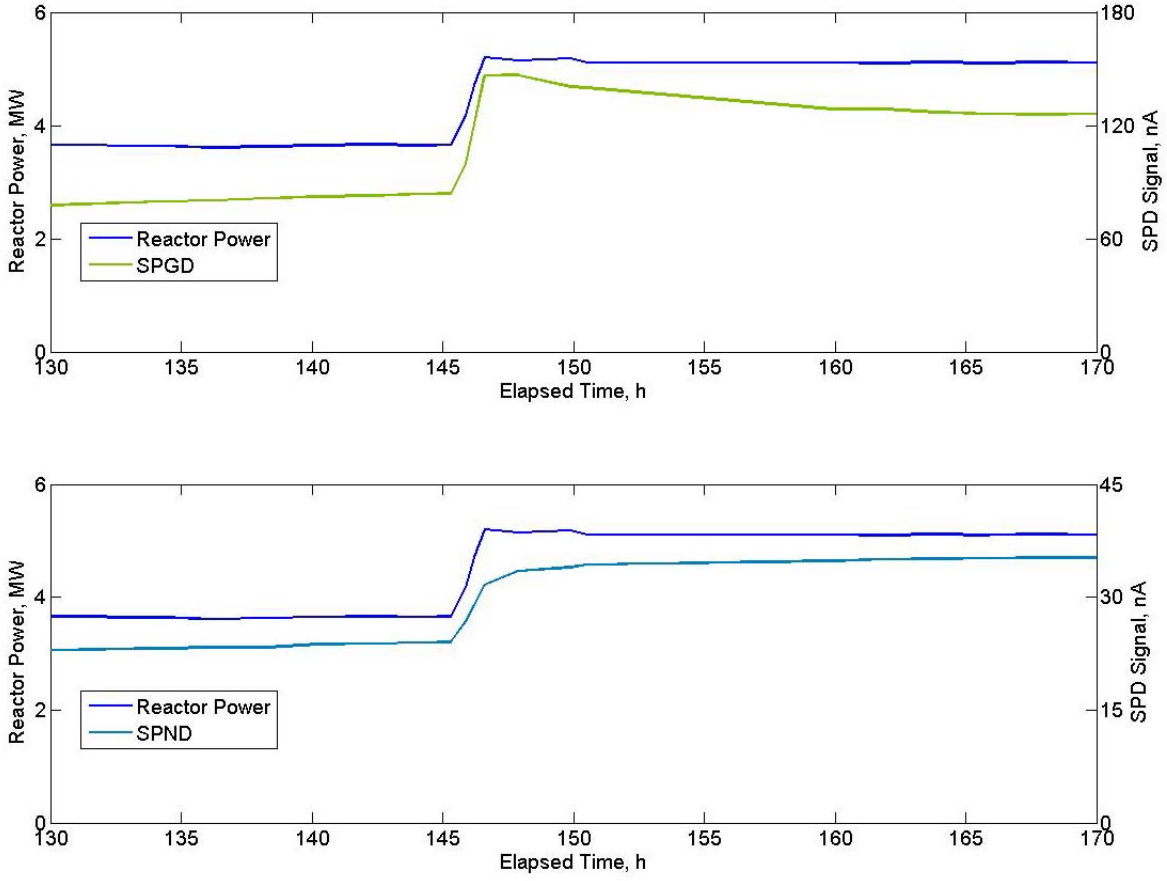

Figure 3-22. SPD signals and reactor power during initial reactor start-up.

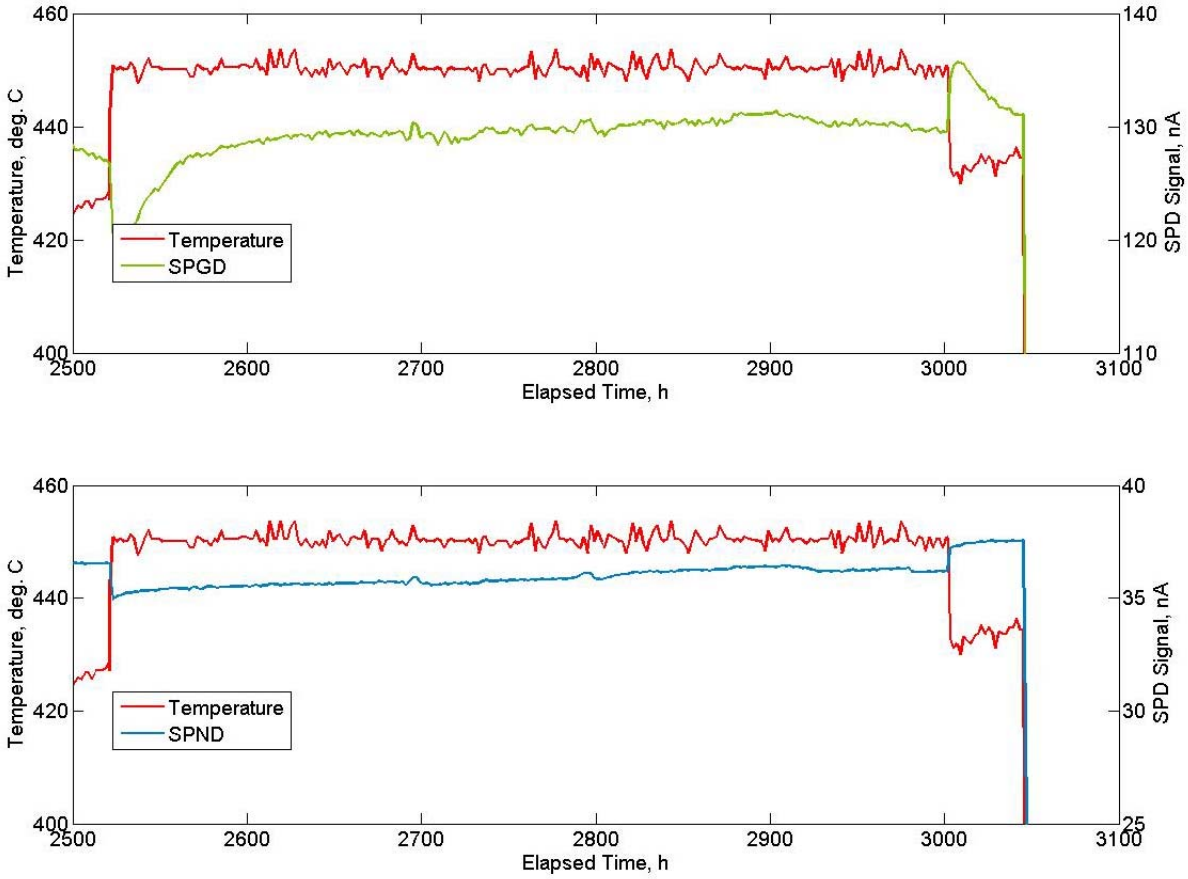

Figure 3-23. Response of SPDs to temperature changes at constant reactor power.

Possible explanations are:

- Changes to neutron spectrum due to injection of neon into the gas gap,[60]
- Increases to the neutron energies as neutrons pass from low temperature coolant to hot graphite due to thermal scattering interactions with graphite,[61] and
- Temperature dependant neutron cross-sections of emitter materials.[61]

Discussions about this phenomena are continuing, and additional evaluations will continue during the remainder of this irradiation.

3.5. Summary

As described in this section, this project completed this task by leveraging its funding with an ATR NSUF-funded ultrasonic transducer irradiation test that is being performed in the MITR. During FY-12 and FY-13, appropriate piezoelectric and magnetostrictive candidate materials were selected. In addition, several other important activities were completed during these initial two years. The irradiation conditions were defined, a well instrumented test capsule was designed, test equipment was acquired, and the test transducers were fabricated and transported to MIT. During FY-14, the test capsule was assembled and installed into the MITR; and the irradiation was started. Results to date of this ongoing irradiation test indicate that transducers fabricated using magnetostrictive alloys (Galfenol, in particular) are very tolerant to neutron and gamma radiation effects and would be good candidates for in-core use. Piezoelectric transducer performance has been less steady, but this may be due to inconsistencies in coupling between the

piezoelectric element and the waveguide (as the coupling is effected by mechanical pressure and can vary greatly during rapid temperature changes). Nonetheless, aluminum nitride has performed well and should be considered a good choice for in-core use. As the irradiation is ongoing, final conclusions cannot be made until the irradiation has finished and PIE of the test transducers and material samples is completed.

4. TASK 2: ULTRASONIC SIGNAL PROCESSING METHODS

Analysis of signals from ultrasonic instruments located within a reactor core is complicated by the extreme environment and a lack of direct access to the system. The ultrasonic transducers may be subjected to extremes in temperature, corrosive environments, flow vibrations, and both neutron and gamma radiation. Even if constructed from materials tolerant to the long term degradation associated with the radiation environment, these conditions can cause increases in signal noise, spurious signal artifacts, and changes to the coupling between the transducer and the system it is interrogating. An improved methodology is needed to mitigate these factors. The objective for Task 2 was to enable enhancement of signal processing methods used to support various types of ultrasonic sensors.

Task 2 was initiated by first completing an extensive background review of the various desired measurement parameters, how those parameters could be measured using ultrasonics, and what signal characteristics could be used to infer the desired information.[13] A strategy for incorporating the different required signal processing methodologies was also developed.

Subsequent work focused on development and demonstration of signal processing method enhancements for ultrasonic thermometry applications. This work relied upon measurements completed using single and multiple segment waveguide type ultrasonic thermometers with magnetostrictive transducers similar in design to those being evaluated in the transducer irradiation test of Task 1. As a first step, INL provided data for development and demonstration of candidate signal processing method enhancements to PNNL and ANL. During FY-15, PSU will use data from the PSU-led MITR irradiation test and PSU-performed elevated temperature tests of magnetostrictive and piezoelectric transducers assess the effects of irradiation and temperature on transducers and waveguides. Identification of gaps in the developed methodology and proposed follow-on work to address these gaps were documented. A flow chart describing this work process is shown in Figure 4-1. Additional details about each activity are reported in this section.

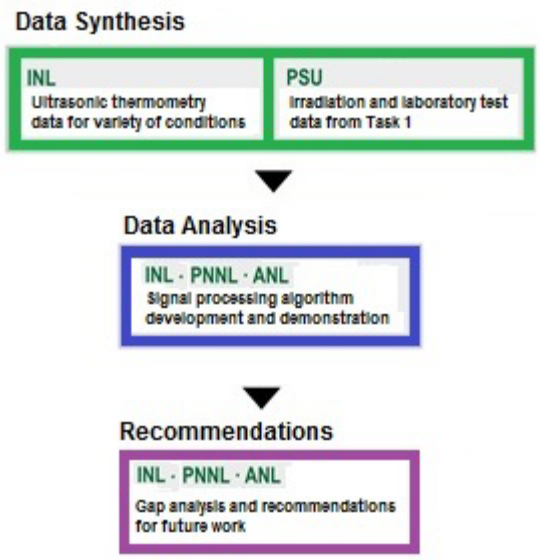

Figure 4-1. Signal processing enhancement project flow chart.

4.1. Ultrasonic Thermometry Data Generation (INL)

As previously noted, INL provided data for development and demonstration of candidate signal processing method enhancements to PNNL and ANL This section provides additional details about the data and how it was obtained.

4.1.1. Ultrasonic Thermometer Test Description

A Matec brand tone-burst signal generation card was used for pulsing and receiving signals to the UT. Input parameters were set to optimize signal strength at room temperature. Received signals were band-pass filtered (low pass frequency of 100 kHz, high pass frequency of 5 MHz) via the Matec control software in order to reduce signal noise. Signals were output to a Tektronix oscilloscope for averaging and data recording. The thermometers were located inside a tube furnace purged with inert gas, as shown in Figure 4-2. A Type-S thermocouple was co-located with the thermometers and used to measure the furnace temperature. All thermometer segments were located in the central isothermal zone of the furnace and are assumed to have been at a uniform temperature. Thermometers were housed in alumina protection tubes for acoustic isolation. Raw waveforms were recorded at increments of 200 ^{O}C for temperatures between room temperature (30 ^{O}C) and 800 ^{O}C.

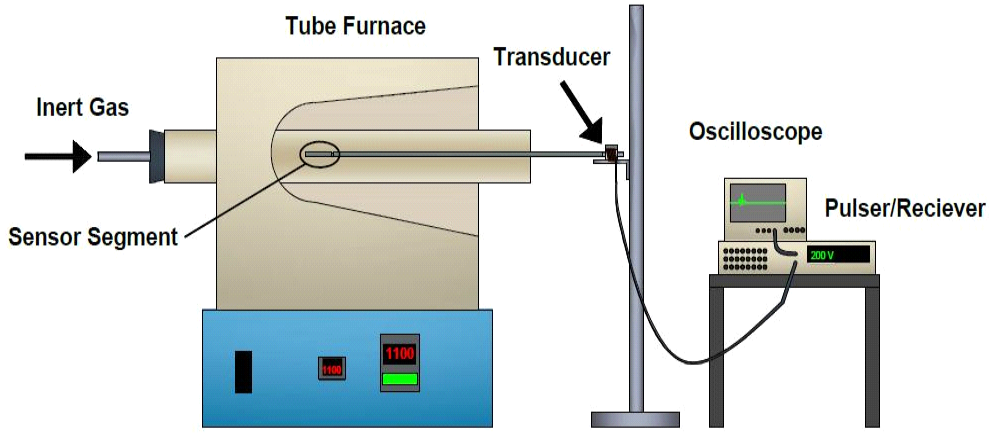

Figure 4-2. Schematic of ultrasonic thermometer test setup.

4.1.2. High Frequency Multi-Segment Thermometer

The high frequency magnetostrictive transducer consists of a coil operating in pulse-echo mode at 1.9 MHz, a Sm-Co biasing magnet, and a segment of 0.254 mm diameter Remendur wire butt-welded to the thermometer waveguide using a laser welder. Damping was achieved by clamping the free end of the Remendur in a vise with fine stainless steel wool. The thermometer consisted of a 0.254 mm stainless steel wire waveguide with reflectors fabricated by laser welding small segments of the same wire to the waveguide, creating small bumps. The UT has three sensor segments formed by the three welded reflectors and the end of the wire. The segments were nominally 15 mm in length. Reflectors were intended to provide a 10% reflection coefficient at room temperature. Features of the thermometer are shown in Figure 4-3.

4.1.3. Low Frequency Single-Segment Thermometer

The low frequency transducer consists of a coil operating in pulse-echo mode at 0.7 MHz, a Sm-Co biasing magnet, and a segment of 0.254 mm diameter Remendur wire butt-welded to the thermometer wave-

guide using a laser welder. Damping was achieved by clamping the free end of the Remendur in a vise with fine stainless steel wool. The thermometer consists of a 0.254 mm stainless steel wire waveguide with a reflector fabricated by laser welding small segments of the same wire to the waveguide, creating a small bump. The UT has one sensor segment formed by the welded reflector and the end of the wire. The segment is nominally 45 mm in length. The reflector was intended to provide a reflection similar in magnitude to the wire end reflection at room temperature. Features of the low frequency thermometer are shown in Figure 4-4.

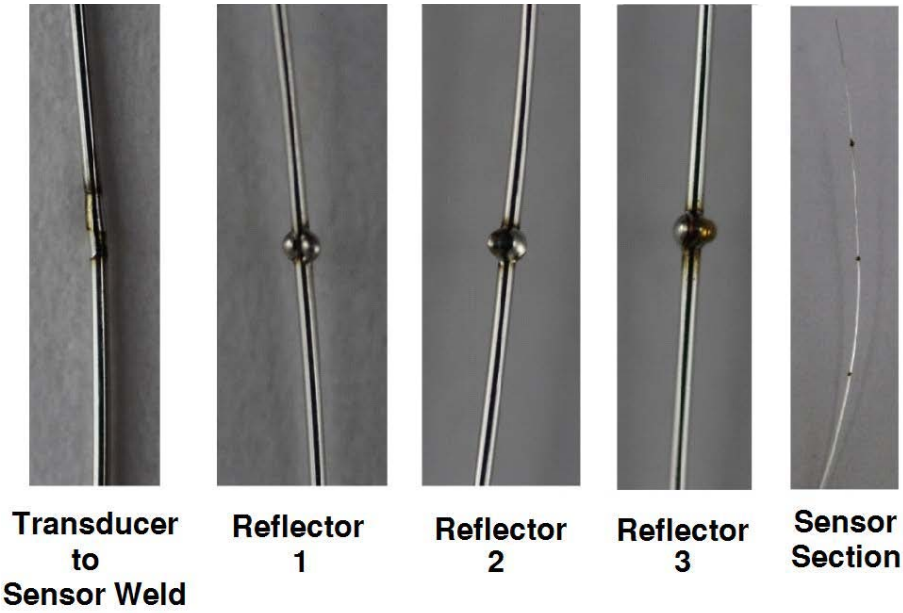

Figure 4-3. High frequency, multi-segment thermometer features.

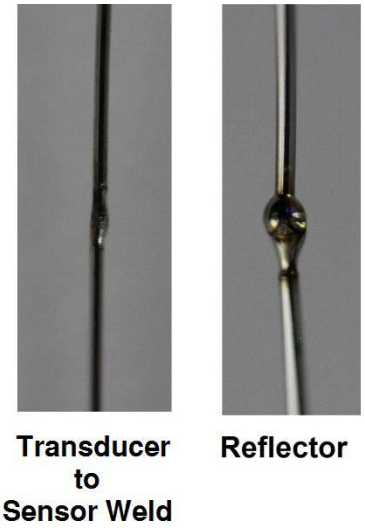

Figure 4-4. Low frequency, single segment thermometer features.

4.1.4. Recorded Signals

Raw waveforms were recorded for each thermometer in both damped and un-damped conditions. The damping reduces unwanted signal artifacts that can interfere with the signals to be processed. However, damping also eliminates higher order reflections that can be used to increase the accuracy of measurements. Figures 4-5 through 4-8 show recorded waveforms captured for each thermometer (damped and un-damped) at room temperature. The primary features of the waveforms are labeled.

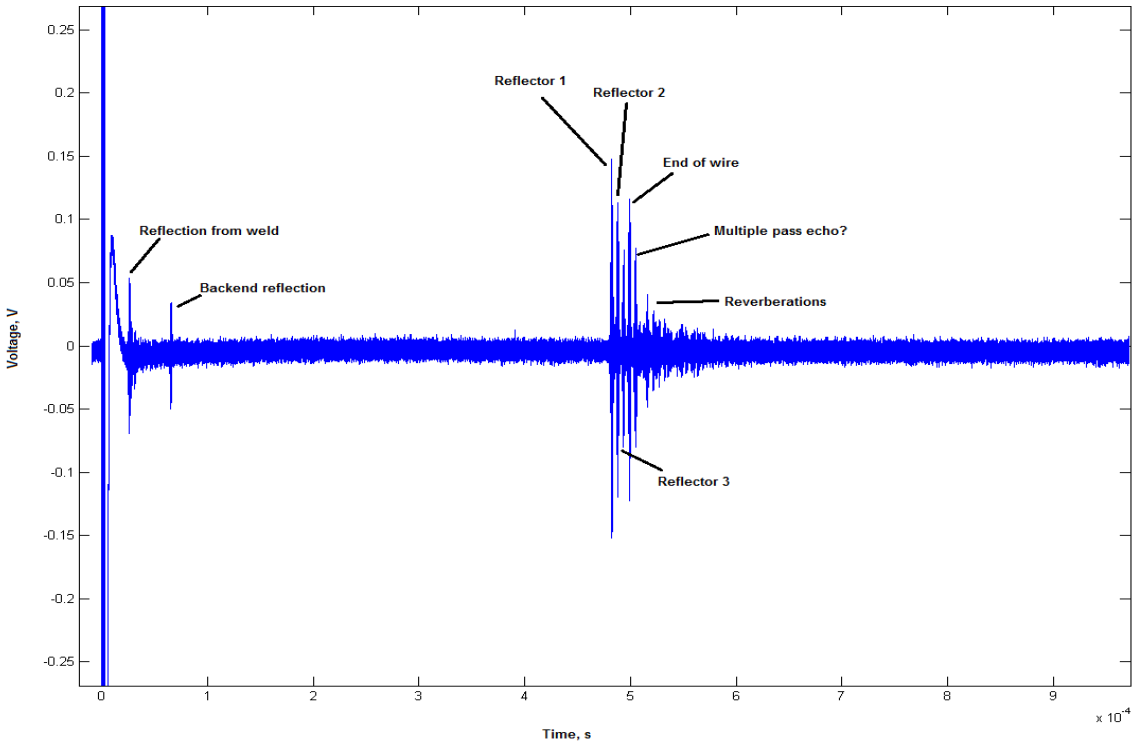

Figure 4-5. Recorded signal for high frequency/multi segment thermometer with damping.

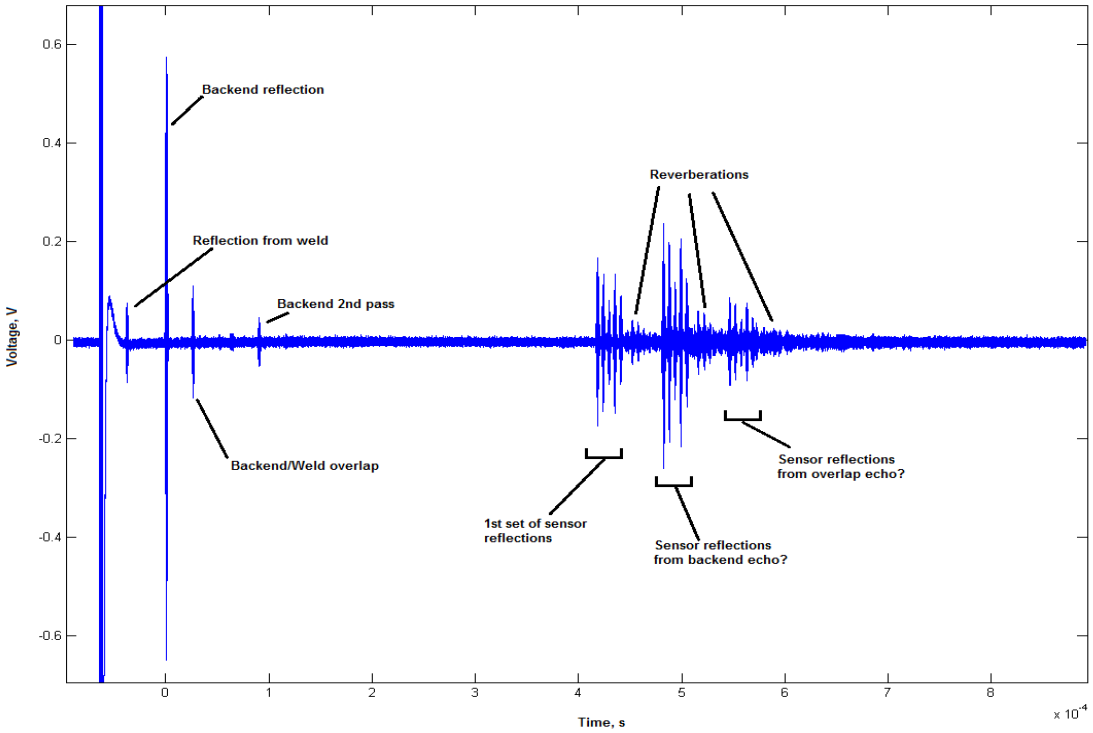

Figure 4-6. Recorded signal for high frequency/multi segment thermometer without damping.

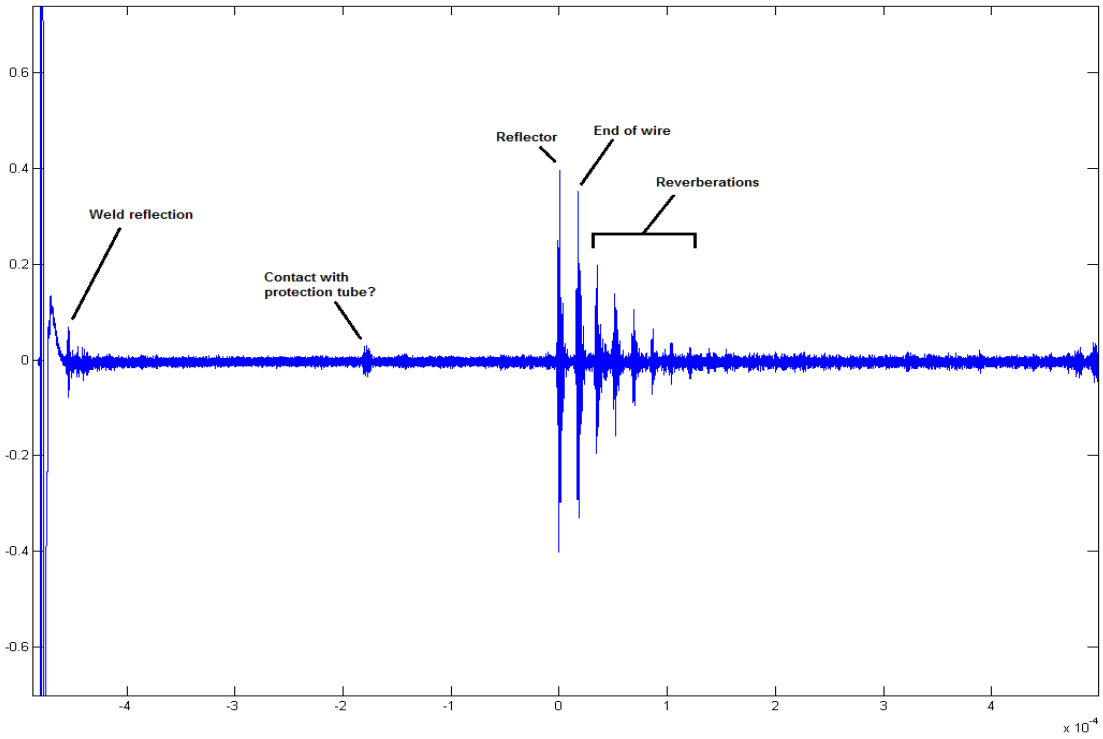

Figure 4-7. Recorded signal for low frequency/multi segment thermometer with damping.

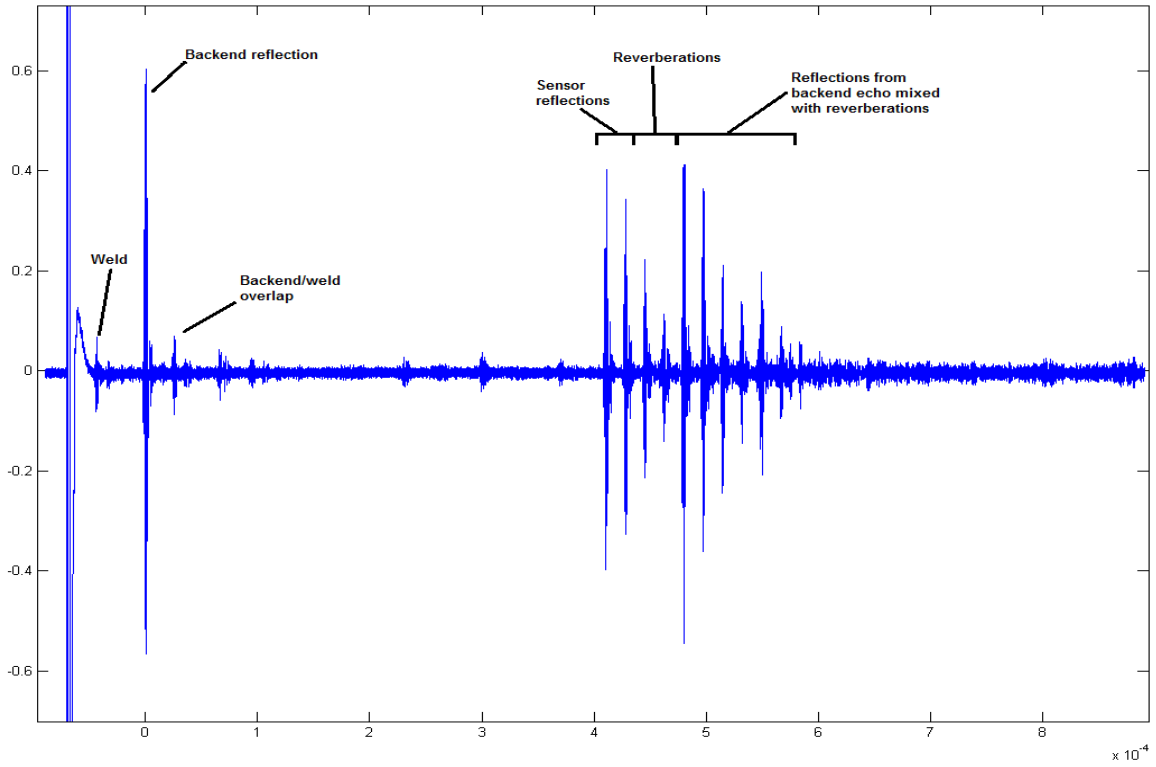

Figure 4-8. Recorded signal for low frequency/multi segment thermometer without damping.

4.2. Signal Processing Method Evaluations (PNNL)

4.2.1. Signal Processing Requirements for Ultrasonic Thermometry

Requirements for ultrasonic thermometry in an in-pile environment are documented in Tables 2-1 and 2-2. They include an accuracy of 2% or better with a spatial resolution of 1-2 cm axially and 0.5 cm radially. These requirements cover both fuel and cladding temperature and encompass ceramic and metallic fuels for Light Water Reactors (LWRs) and Sodium Fast Reactors (SFRs). Note that a variety of requirements for other ultrasound-based sensors are also defined, including sensors for measuring pressure, fission gas release, fuel and cladding dimensional changes, and morphology changes.

4.2.2. Sources of Uncertainty

From an ultrasonic measurements perspective, the key parameters that are measured are:

- Time-of-flight (or equivalently, sound speed), including its variation as a function of frequency,
- Attenuation and signal amplitude, and
- Frequency content, including the presence of harmonics.

For thermometry, the focus of measurements is on time-of-flight as this parameter, which depends on sound speed, varies with temperature. Estimation of the time-of-flight requires the detection of individual acoustic wave packets that are reflected from the reflectors or welds on the waveguides.

A multiplicity of factors combines to reduce the accuracy of time-of-flight measurements in ultrasonic thermometry. These include measurement noise, attenuation, dispersion, and the effects of temperature and radiation on the transducer material itself. Attenuation and dispersion effects may occur in both the

cabling and the acoustic wave propagation in the waveguide. Additional uncertainty is introduced through imprecision in locating the reflectors and the potential presence of additional wave modes.

4.2.3. Assumptions

Within the context of this work, the following assumptions are made:

- Ultrasonic measurements are acquired using a computer-controlled data acquisition system,
- The measurements will be processed in an automated fashion, to extract one or more of the parameters listed above, and
- Ultrasonic thermometer fabrication is precisely controlled and introduces little to no uncertainty in the measurement. As such, all sources of uncertainty from the fabrication process can be ignored.

4.2.4. Analysis Approach Summary

Multiple approaches to analysis were utilized, with the goal of improving SNR as a first step to identifying acoustic wave packets and computing time-of-flight. Prior to analysis, theoretical calculations were performed to obtain a precise theoretical value of wave speed and attenuation that were based on acoustic dispersion curve analysis. The dispersion curve relates wave speed (group velocity) to the frequency of the acoustic wave and the dimensions of the waveguide. These theoretical values provide bounds on the quantities of interest and are used in the analysis algorithms summarized below.

Analysis algorithms include:

- *Time-domain Analysis:* Based on theoretical values of wave speed, and available ultrasonic thermometer design data, time gates may be identified where signals of interest are expected. These gates help in eliminating non-relevant signals for further analysis. In addition, common temporal-domain analysis techniques involve correlation of the time series under investigation with a known time series or performing peak detection and measuring peak-to-peak time (which provides information on time-of-flight). Also, a time series can be correlated with itself with or without offset to produce an auto-correlation function. The time-offset will reveal repeating structures in the time series coming from different reflected signals and is a mechanism for improving the accuracy of time-of-flight computations.
- *Frequency-domain Analysis:* There are several ways to analyze data in the frequency domain. These involve some sort of spectra analysis and can use Fourier, cosine, wavelet transforms or some other form of time-domain to frequency-domain transform. In this task, Fourier transforms are used to produce power spectrum and spectrograms. The latter tries to combine features of both time-domain analyses with frequency-domain analysis.
  - *Filtering:* A suite of standard frequency filters may be applied to eliminate all responses outside the bandwidth of the probe. Additional band-pass filters may be used to focus on signals containing a narrow band of frequencies. By using a number of such narrow-band filters, a decomposition of the measured signal into its constituent frequency components and their behavior over time, may be identified. Such analysis is often used to reduce the effects of noise.
  - *Time and frequency based analysis:* The spectrogram is a common visual analysis method for examining temporal signals by simultaneously viewing them jointly in the time and frequency domain. It is used to visualize both the temporal-domain and frequency-domain features in the data to find salient patterns by visual inspection. It is most commonly used in speech analysis. In a spectrogram, the horizontal axis represents time; and the vertical axis represents frequency. The strength of a given frequency in the spectrogram is indicated by the color or brightness of the spectrogram at the given time and frequency. A spectrogram generated from one data set is shown in Figure Figure 4-9. This figure illustrates how a spectrogram can be used aid in identifying a reflection peak.

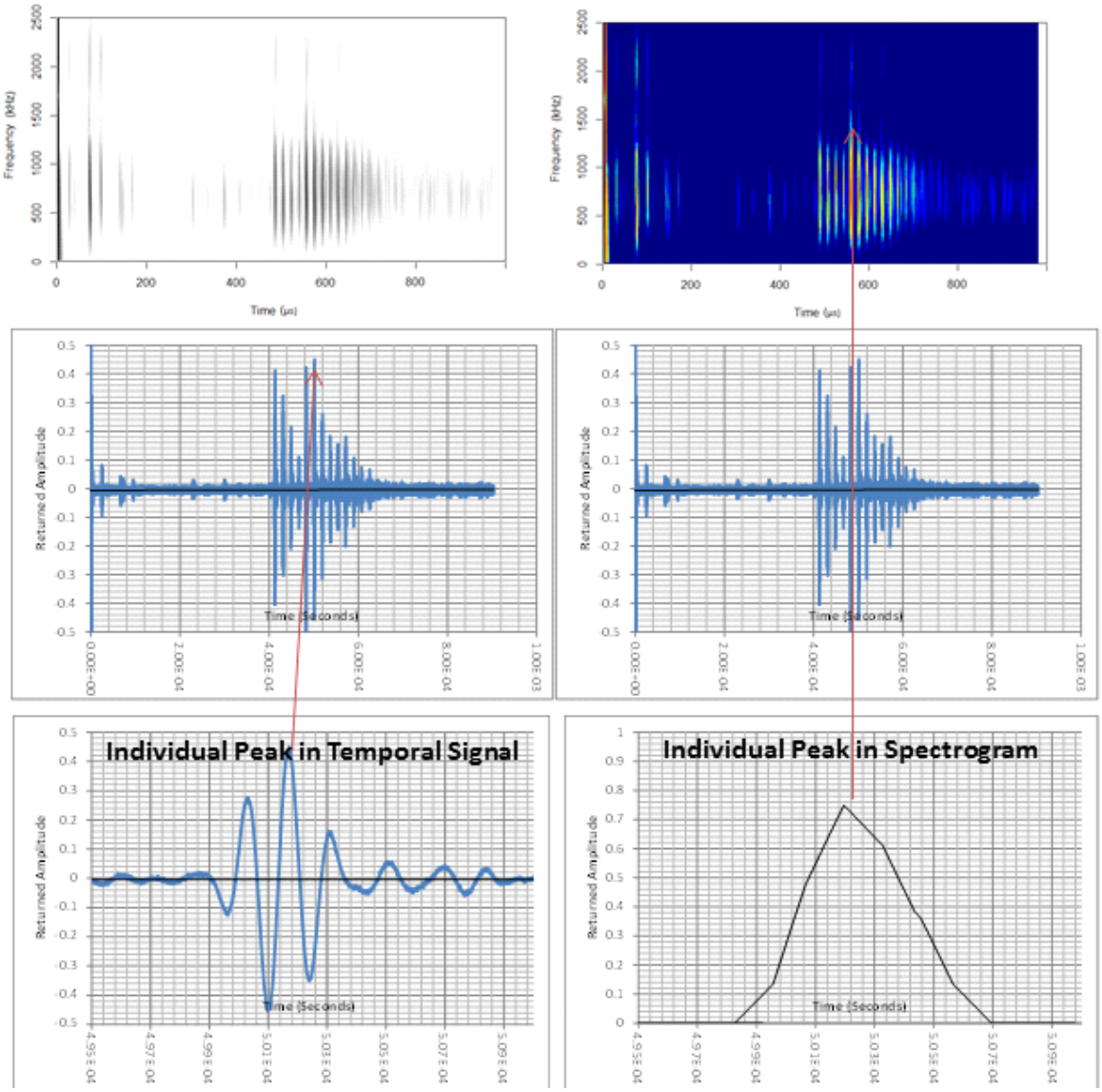

Figure 4-9. Spectrogram of a returned signal along with the temporal signal and illustrations of both an individual reflection peak and the associate peak in the spectrogram.

The size of the Fourier analysis window of the spectrogram sets the different levels of frequency and time resolution that can be achieved in the spectrogram. A long time window will resolve frequency at the expense of time. This results in a narrow band spectrogram showing individual harmonics (component frequencies) but also smears together adjacent 'moments'. If a short time analysis window is used, adjacent harmonics are smeared together; but better time resolution is achieved which results in a wide band spectrogram where salient frequencies appear as vertical lines or striations in the spectrogram. This can add complexity to the analysis task since the analysts must make decisions on proper settings for the time and frequency windows.

Figure 4-10 shows the calculated acoustic velocity as a function of temperature for the four conditions (High Frequency, Low Frequency, Damping, and No Damping), based on time domain analysis. Available data were time-gated and auto-correlated; and a peak-finding algorithm was employed to identify relevant signal peaks. The time-of-flight was computed as the difference in arrival times between successive peaks.

The time-of-flight between successive peak pairs was averaged, and the standard deviation computed. The ratio of standard deviation to mean of the peak-to-peak separation gives an estimate of the temporal resolution. The acoustic velocity is computed by using the time-of-flight with the separation distance between the corresponding reflectors on the thermometer.

The two types of probes (high frequency and low frequency) used different geometries for the experiment with two weld points separated by 45 mm for the low frequency (0.7 MHz) experiments and three weld points separated from each other by 15 mm for the high frequency (1.9 MHz) experiments. Table 4-1 gives the results of measuring multiple returned peaks and determining the peak-to-peak separation in time. Table 4-2 shows the results in terms of velocity and the associated uncertainty.

Acoustic velocity in steel generally decreases as temperature increases due to a number of mechanisms. As seen from the calculated ultrasonic velocities, this trend is evident in the data. In addition, a clear separation is seen between data from the high frequency probe (upper curves) and low frequency data (lower curves). In each case, the velocity at room temperature is consistent with theoretical values computed from dispersion analysis.

In addition to intrinsic change in acoustic velocity due to temperature, thermal expansion of the waveguide is expected to add to uncertainty in acoustic velocity calculation, albeit by a very small amount. To determine the level of uncertainty due to thermal expansion, the change in length was computed using tabulated values from the literature of the coefficient of thermal linear expansion for steel. acoustic velocity values, after correction for thermal expansion, are presented in Figure 4-11, along with the related uncertainty values.

Table 4-1. Mean time between returned peaks ‘μ’ along with standard deviation ‘σ’ and the ratio of standard deviation to mean ‘σ/μ’ as an indicator of temporal resolution.

Condition	Statistic	21.8°C	200.5°C	409.0°C	606.8°C	805.5°C
Low Frequency with Damping	μ	1.72E-05 s	1.79E-05 s	1.87E-05 s	1.97E-05 s	2.04E-05 s
	σ	2.39E-07 s	2.37E-07 s	1.89E-07 s	2.27E-07 s	4.28E-07 s
	σ/μ	1.39%	1.32%	1.01%	1.16%	2.10%
Low Frequency without Damping	μ	1.73E-05 s	1.77E-05 s	1.87E-05 s	1.95E-05 s	2.06E-05 s
	σ	2.60E-07 s	5.45E-07 s	1.95E-07 s	2.07E-07 s	2.21E-07 s
	σ/μ	1.50%	3.09%	1.04%	1.06%	1.07%
High Frequency with Damping	μ	5.61E-06 s	5.77E-06 s	6.02E-06 s	6.30E-06 s	6.74E-06 s
	σ	6.25E-08 s	1.80E-07 s	3.71E-08 s	1.76E-07 s	3.59E-07 s
	σ/μ	1.11%	3.11%	0.62%	2.79%	5.33%
High Frequency without Damping	μ	5.57E-06 s	5.84E-06 s	6.06E-06 s	6.32E-06 s	6.58E-06 s
	σ	9.31E-08 s	2.55E-07 s	7.63E-08 s	1.10E-07 s	1.83E-07 s
	σ/μ	1.67%	4.37%	1.26%	1.75%	2.78%

Table 4-2. Velocity resolution as a function of temperature and experimental condition (Low Frequency, High Frequency, With Damping, Without Damping)

Condition	21.8°C	200.5°C	409.0°C	606.8°C	805.5°C
Low Frequency with Damping	5220 ± 72.4 m/s	5020 ± 66.3 m/s	4820 ± 48.9 m/s	4580 ± 53.0 m/s	4410 ± 92.4 m/s
Low Frequency without Damping	5200 ± 78.2 m/s	5100 ± 157 m/s	4820 ± 50.4 m/s	4615 ± 48.9 m/s	4370 ± 46.9 m/s
High Frequency with Damping	5350 ± 59.6 m/s	5200 ± 162 m/s	4980 ± 30.7 m/s	4760 ± 133 m/s	4450 ± 237 m/s
High Frequency without Damping	5390 ± 90.1 m/s	5140 ± 224 m/s	4950 ± 62.4 m/s	4750 ± 83.0 m/s	4560 ± 127 m/s

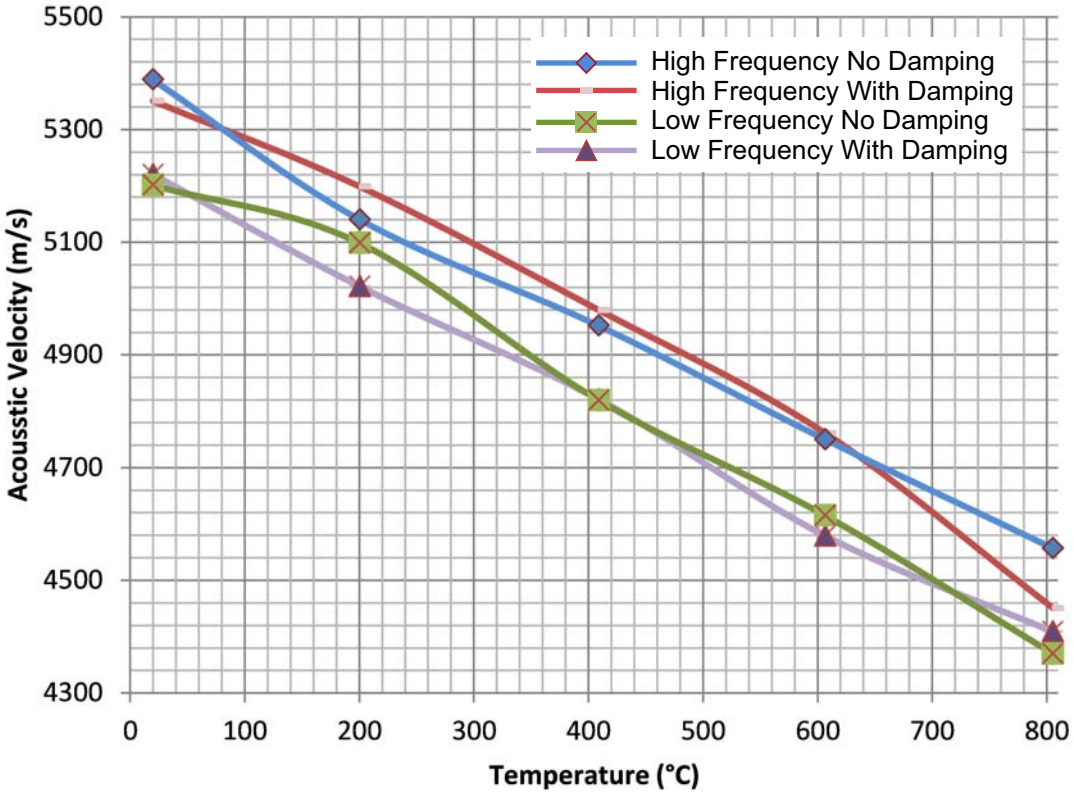

Figure 4-10. Acoustic velocity as a function of temperature.

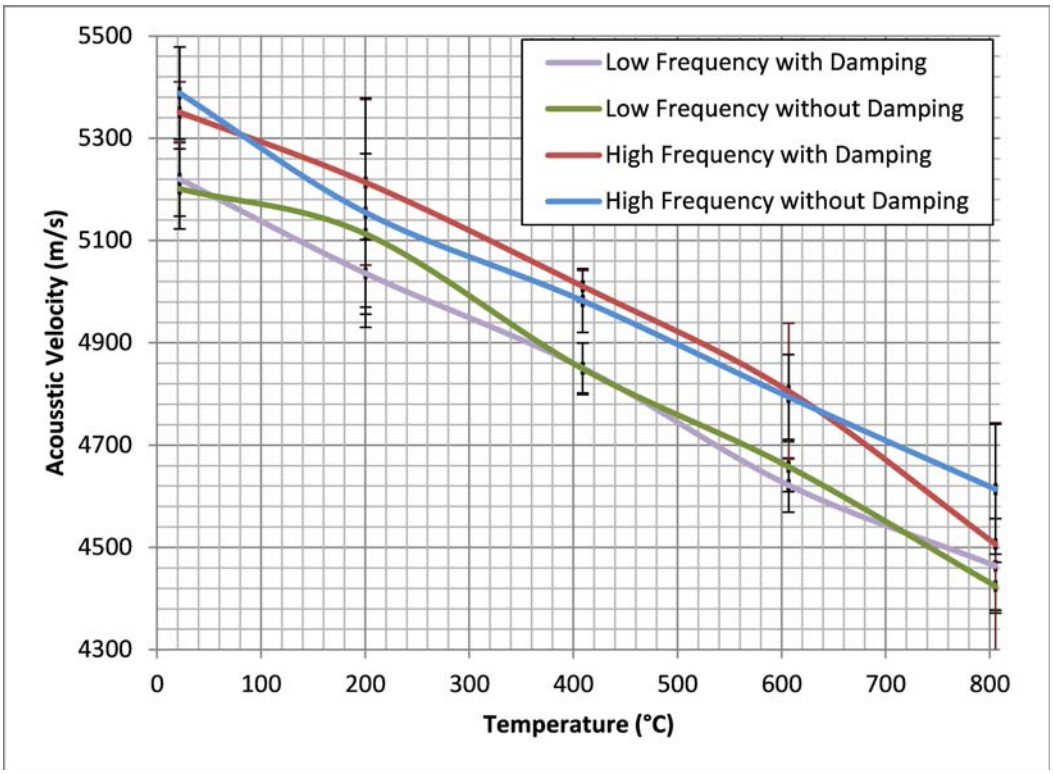

Figure 4-11. Acoustic velocity as a function of temperature after correction for thermal expansion.

4.2.5. Analysis Approach Results

The comparison of the results from the three domains showed that the time-domain processing produced the best estimate of temperature resolution but was only slightly better than the other two processing domains. The results show that the time resolution is generally within a range of 1-2% in most of the scenarios analyzed. This produces a sound velocity resolution of approximately 100 m/s. Due to the limited number of peaks in each data set, estimation of the temperature resolution yielded a fairly course resolution of 46°C based on one standard deviation from mean. Additional experimental runs should improve this resolution estimate.

4.2.6. Recommended Additional Work

In terms of the signal processing efforts, the most important recommendation would be to generate more experimental data to reduce the estimation error to improve both spatial and temperature resolution estimations. Other important recommendations include implementing adaptive filtering techniques to reduce noise and aid in the discernment of propagation modes.

4.3. Demonstration of Automated Signal Processing Method (ANL)

4.3.1. Development of Signal Processing Algorithm for Ultrasonic Thermometer Applications

Argonne National Laboratory (ANL) has developed a MATLAB® based package, called imagingGUI, as a base to explore advanced Non-Destructive Testing (NDT) solutions or to develop advanced data analysis and signal process algorithms. This approach offers the capability of system integration and control, provides flexibility for adding customized software, allows cross-linking between different platforms, enhances data and sensor fusion, and saves software developing time and cost. To characterize parameters

from in-pile ultrasonic thermometry, a plug-in toolbox was developed and integrated into the imagingGUI package. It can be easily adapted to a LabView® platform for real-time characterization. The toolbox will generate and display an envelope of the ultrasonic radio frequency (RF) signal for high-accuracy time-of-flight measurements of the reflectors and the end of the rod and then estimate the temperatures of each section of the rod. Figure 4-12 displays the data of one of the INL ultrasonic thermometry data samples. The right window shows the file information, signal process parameters, calculated time-of-flight and speed-of-sound, and estimated temperatures each section. The left displays the ultrasonic RF signal overlapped with an envelope calculated.

The envelope is generated by using the Hilbert transformation and smoothed with the moving average technique (default: 10-point moving average). The times-of-flight are calculated according to the two input parameters, reflector spacing, and peak detection threshold. The speed-of-sound is estimated based on an empirical equation of sound-velocity-to-temperature, shown in Equation 4-1, for the SS304 ultrasonic thermometer fabricated by INL:[62]

$$c = 0.000134 \cdot T^2 - 1.14 \cdot T + 5222.77 \quad (4\text{-}1)$$

where c is the speed-of-sound in m/s, and T is the temperature in degrees Celsius.

The procedures for the signal process are listed as the following:

1. Select a data file;
2. Automatically read and display the file information and the RF signal data;
3. Automatically generate and display an envelope of the RF signal;
4. Input two parameters, reflector spacing and peak detection threshold
5. Automatically calculate and display time-of-flight of reflectors and the end of the thermometer rod;
6. Automatically estimate and display temperature of each section of thermometer rod;

INL provided a set of data for low-frequency, single-segment and high-frequency, multi-segment rods, respectively, with various operation temperatures. A separate file was created for each test and saved in CSV format.

4.3.2. Low Frequency, Single Segment Thermometer Results

An analysis of the data for the low frequency, single segment rod was conducted using the new imaging-GUI toolbox developed by ANL for ultrasonic thermometry applications. Figure 4-13 shows a RF pulse train that contains reflections from the reflector and the end of the rod, and the multiple reflections between them at 800 ^{o}C. An envelope of the pulse train is calculated and overlapped with the pulse train. Figure 4-14 shows the speed-of-sound calculated from the equation and experimental data, respectively. Differences may be due to the empirical equation being developed for a wire that had been heated for one cycle prior to data collection and the wire used for these tests had not been previously heated.

4.3.3. High Frequency, Multi-Segment Thermometer Results

Figure 4-15 shows the RF pulse trains that contain reflections from the three reflectors and the end of the rod, and the higher order reflections without damping at 400 ^{o}C. Figure 4-16 shows the RF pulse train that contains reflections from the three reflectors and the end of the rod with damping at 200 ^{o}C. The damping setup efficiently damped out the second pulse train. However, the second pulse train does not significantly affect the measurement of temperature of each section. Envelopes of these pulse trains were calculated and overlapped with the pulse trains. Figure 4-17 shows the speed-of-sound calculated from the equation and experimental data, respectively. The results of speed-of-sound are worse than the single segment case simply because the same empirical equation used was for a wire that had been heated for one cycle prior to

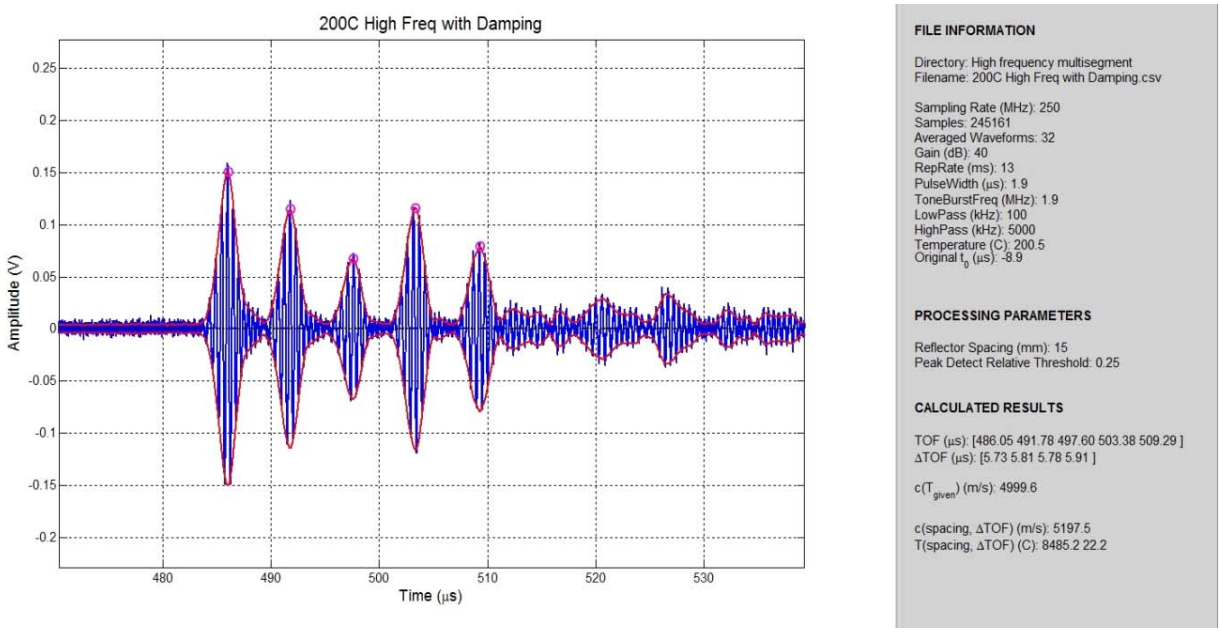

Figure 4-12. Argonne imagingGUI for uploading and analysis of ultrasonic thermometry data.

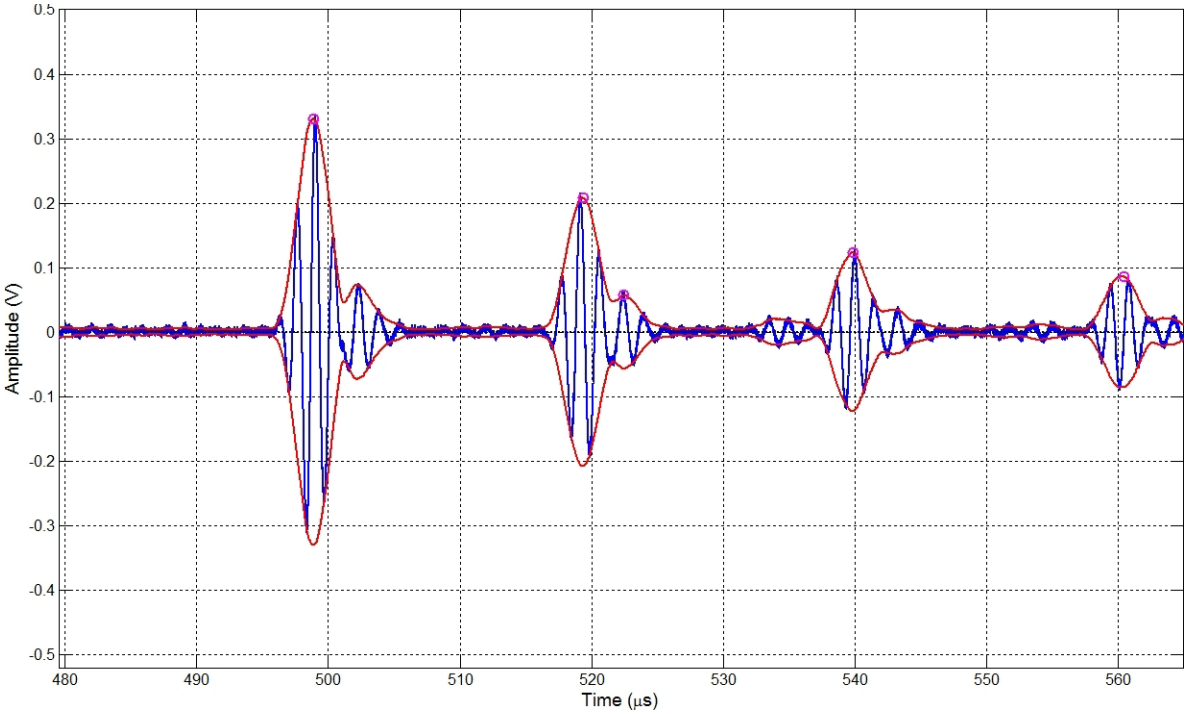

Figure 4-13. Recorded ultrasonic signal and envelop for a single segment thermometer at 800 ^{O}C without damping.

data collection and was obtained using a lower frequency coil (e.g., the speed-of-sound is dependent on frequency).

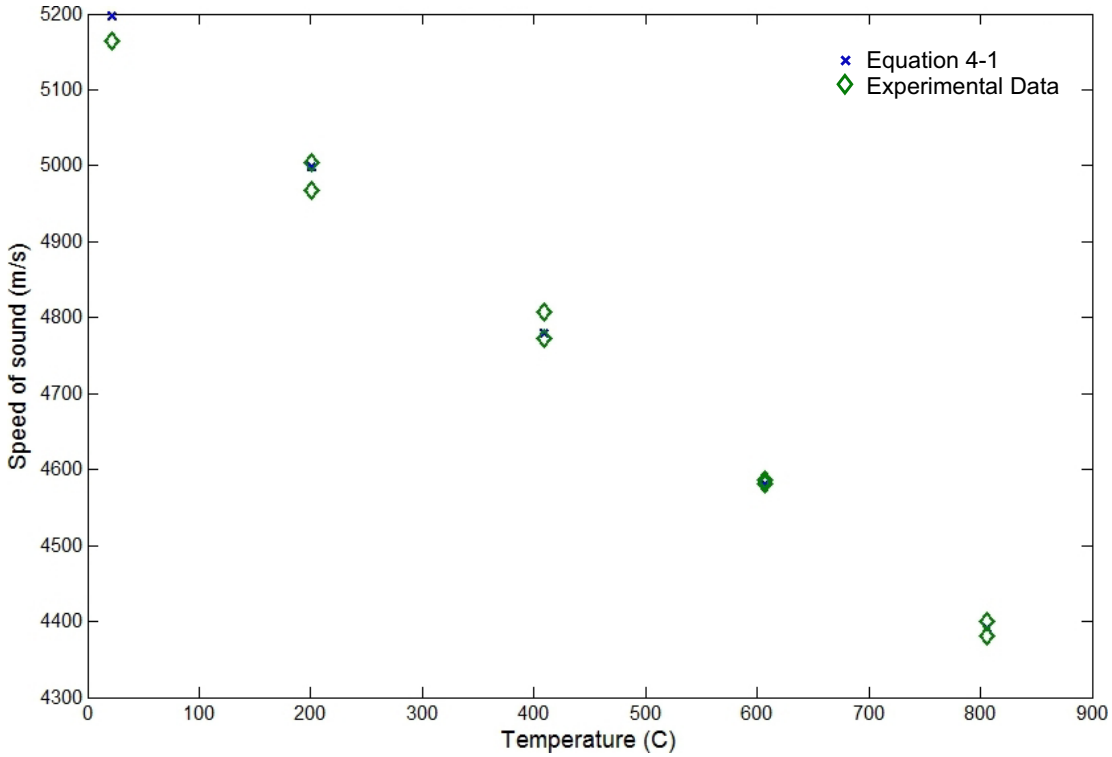

Figure 4-14. Ultrasonic speed-of-sound for a single segment thermometer at various temperatures.

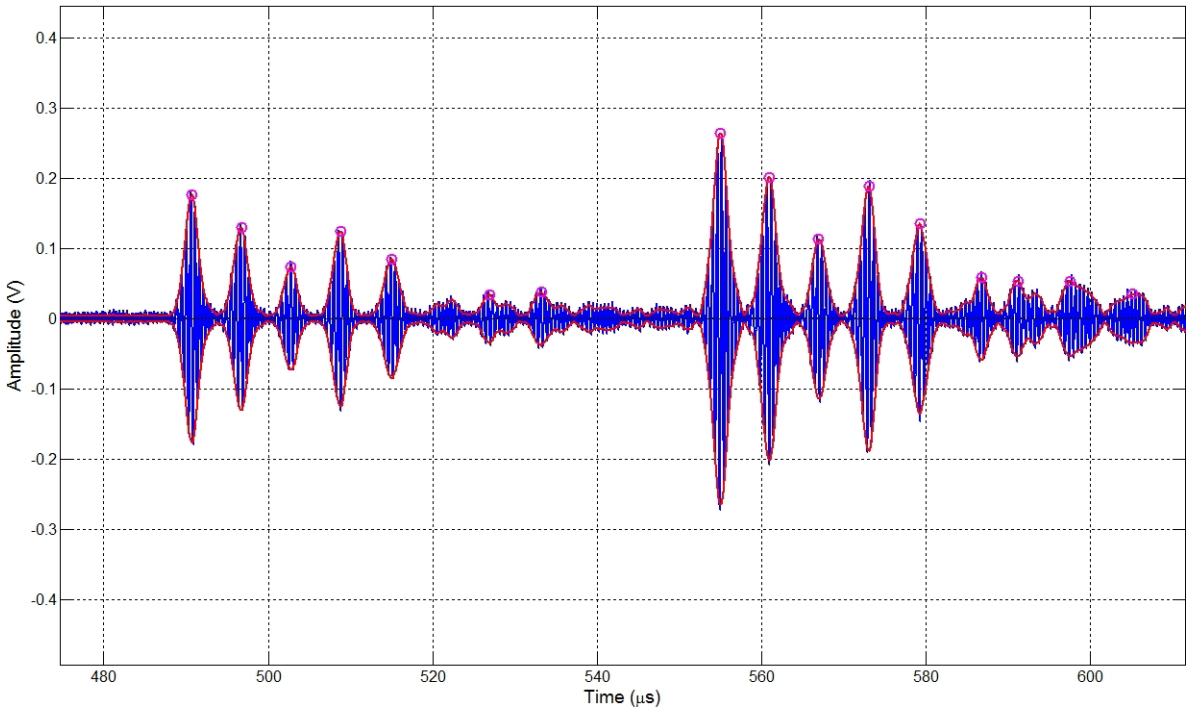

Figure 4-15. Received ultrasonic signal and envelop for a multi-segment thermometer at 400 ^{O}C without damping.

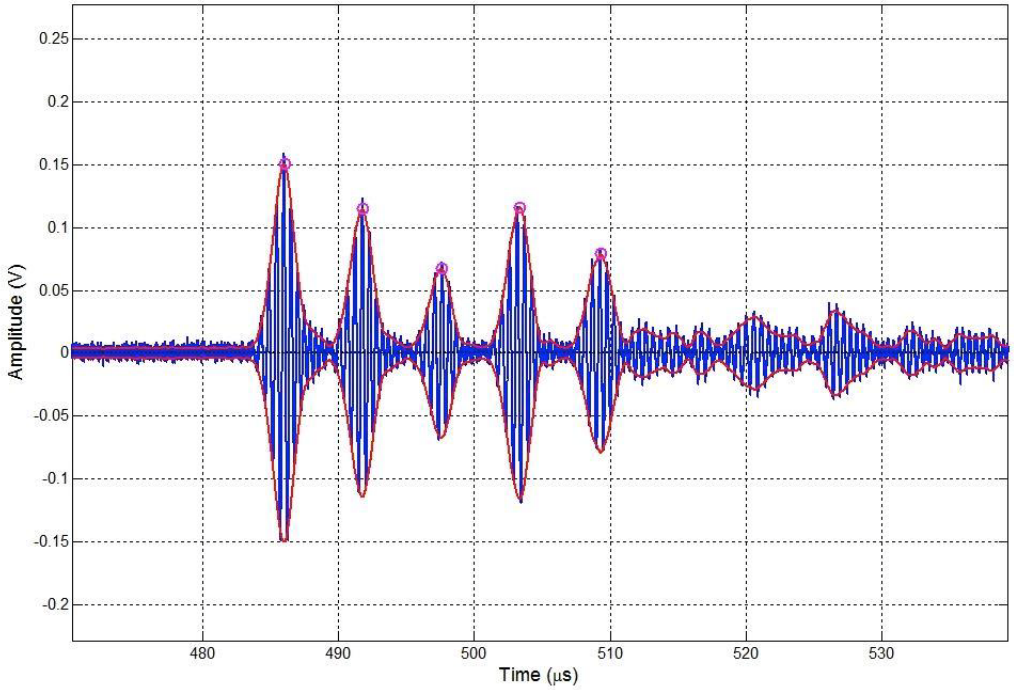

Figure 4-16. Received ultrasonic signal and envelop for a multi-segment thermometer at 200 ^{o}C with damping.

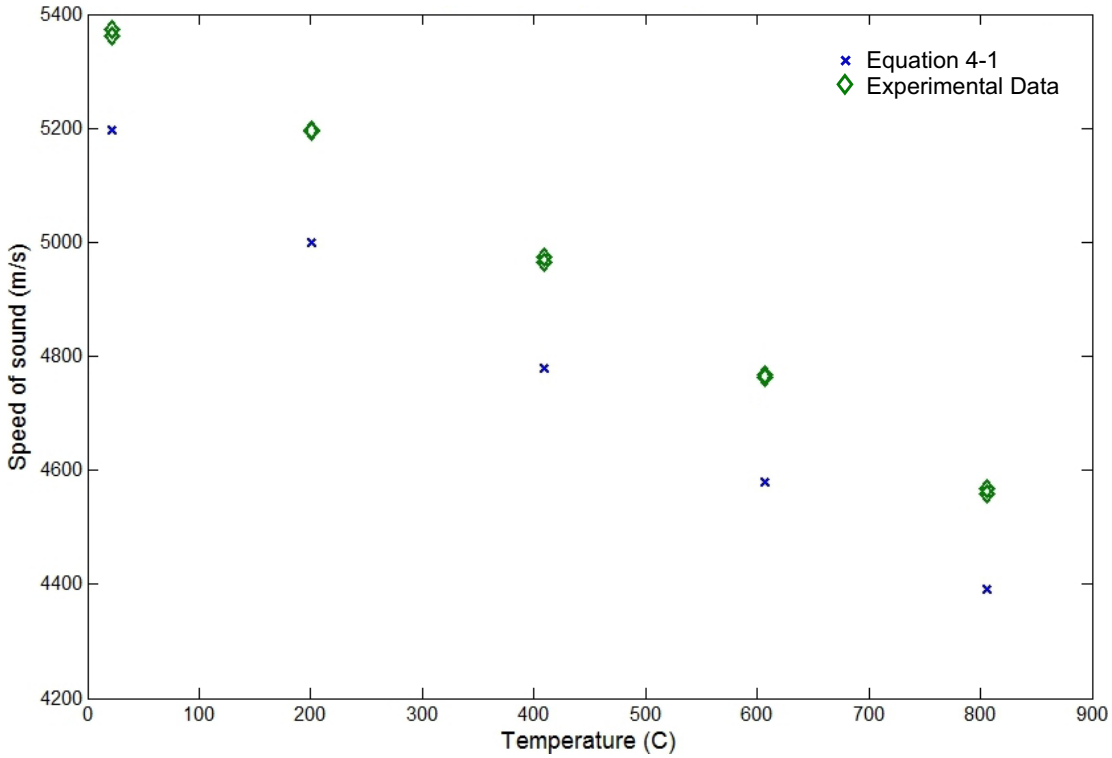

Figure 4-17. Ultrasonic speed-of-sound for a multi-segment thermometer at various temperatures.

4.3.4. Automated Signal Processing Results

Demonstration of an automated data processing package was successful, but differences in velocities calculated from data collected for this effort and data collected during prior testing for the same material, with a different process history, indicate that ultrasonic thermometers must be calibrated individually.

4.4. Summary

One factor limiting the application of ultrasound-based sensors to in-core testing is the need for enhanced signal analysis algorithms applicable to the range of measurable parameters. As a first step in addressing this need, enhanced methods of analyzing data from an ultrasonic thermometer (likely to be the first in-core ultrasonic sensor) were evaluated. To this end, a series of representative ultrasonic thermometer data were produced. In these evaluations, potential methods of analysis were compared and tested. In addition, an automated signal analysis package was demonstrated.

Results indicate that time-domain processing produces the best estimate of temperature resolution, though only slightly better than frequency or time-frequency based analysis methods. Time resolution was generally found to be within a range of 1-2%, producing a sound velocity resolution of approximately 100 m/s. Due to the limited data set, temperature resolution was estimated to be 46°C based on one standard deviation from mean. This resolution estimate can be improved with increased by using larger data sets for analysis. Demonstration of an automated data processing package was successful, but differences in velocities calculated from data collected for this effort and data collected during prior testing for the same material, with a different process history, indicate that ultrasonic thermometers must be calibrated individually. This will ensure that differences due to variations in materials and fabrication processes have minimal effect on measurement accuracy.

5. SUMMARY

Several programs funded by the Department of Energy Office of Nuclear Energy (DOE-NE), such as the FCRD, ARC, LWRS, and NGNP programs, are investigating the use of new fuels and materials for advanced and existing reactors. A key objective of such programs is to understand the performance of these fuels and materials during irradiation. The NEET ASI in-pile instrumentation development activities are focused upon addressing cross-cutting needs for DOE-NE irradiation testing by providing higher fidelity, real-time data, with increased accuracy and resolution from smaller, compact sensors that are less intrusive.

Ultrasonic technologies offer the potential to measure a range of parameters during and after irradiation, including geometry changes, temperature, crack initiation and growth, gas pressure and composition, and microstructural changes under harsh irradiation test conditions. There are two primary issues that currently limit in-pile deployment of ultrasonic sensors. The first is transducer survivability. The ability of ultrasonic transducer materials to maintain their useful properties during an irradiation must be demonstrated. The second issue is signal processing. Ultrasonic testing is typically performed in a lab or field environment, where the sensor and sample are accessible. The harsh nature of in-pile testing and the variety of measurements that are desired demand that an enhanced signal processing capability be developed to make in-pile ultrasonic sensors viable. To address these issues, the NEET ASI program funded a three year the Ultrasonic Transducer Irradiation and Signal Processing Enhancements project, which is a collaborative effort between the Idaho National Laboratory, the Pacific Northwest National Laboratory, the Argonne National Laboratory, the Pennsylvania State University, and the Commissariat à l'énergie atomique et aux énergies alternatives.

As discussed within this document, the two primary objectives of this project, to assess the survivability of ultrasonic transducers and to evaluate enhanced signal processing methods, were successfully completed.

5.1. Irradiation Test

The objective for Task 1 of this project is to evaluate the performance of ultrasonic transducer materials in high flux/high temperature irradiation environments and identify promising materials that will enable development of ultrasound based sensors and systems. Task 1 of this project leverages ATR NSUF funded efforts to develop a test capsule design and define irradiation conditions for evaluating most promising candidate piezoelectric and magnetostrictive transducer materials and designs. From the onset of this effort, an instrumented lead test was proposed, such that real time signals are received from the transducers being tested. Collecting real time signals data allows researchers to accurately measure of the performance and possible degradation of candidate transducer and sensor materials under irradiation.

An in-depth review of prior piezoelectric and magnetostrictive transducer irradiations was used to develop a list of candidate materials for irradiation evaluation. In addition, a design for an instrumented-lead irradiation test capsule and a test plan for evaluating ultrasonic transducer materials were developed, test equipment was acquired, and the test transducers were fabricated and transported to MIT. During FY-14 the test capsule was assembled and installed into the MITR, and the irradiation has started. At the time of this report (September 2014), the fast neutron fluence accumulated in the test rig is 4.1×10^{20} n/cm^2. At this time, irradiation test data indicate that transducers fabricated using magnetostrictive alloys are tolerant to neutron and gamma radiation effects experienced during the first 5000 hours of exposure, and would be good candidates for in-core use. Piezoelectric transducer performance has been less steady, but this may be due to inconsistencies in coupling between the piezoelectric element and the waveguide (as the coupling is affected by mechanical pressure and can vary greatly during rapid temperature changes). Nonetheless, aluminum nitride has performed well and should be considered a good choice for in-core use. As the irradiation is ongoing, final conclusions cannot be made until the irradiation has finished and PIE of the test transducers and material samples is completed.

5.2. Signal Processing Development

The objective for Task 2 was to enable enhancement of signal processing methods used to support various types of ultrasonic sensors in order to mitigate the effects of the in-core environment on measured signals. Initial work on Task 2 focused on completing an extensive background review of the various desired measurement parameters, how those parameters could be measured using ultrasonics, and what signal characteristics could be used to infer the desired information.[13] A strategy for incorporating the different required signal processing methodologies was also developed.

Subsequent work focused on development and demonstration of signal processing method enhancements for ultrasonic thermometry applications. A series of representative ultrasonic thermometer measurements were produced at INL using both single and multiple segment waveguide type ultrasonic thermometers based on magnetostrictive transducers similar to those being evaluated in the transducer irradiation test. Both time-domain and frequency-domain signal processing methods were performed to extract the time-of-flight data from the voltage versus time measurements. Results indicate that time-domain processing produces the best estimate of temperature resolution, though only slightly better than frequency or time-frequency based analysis methods. Changes in the time-of-flight (or speed-of-sound) were used to determine the measured temperature. Demonstration of an automated data processing package was successful, but differences in velocities calculated from data collected for this effort and data collected during prior testing for the same material, with a different process history, indicate that ultrasonic thermometers must be calibrated individually. This will ensure that differences due to variations in materials and fabrication processes have minimal effect on measurement accuracy.

5.3. Key Observations and Recommendations for Future Work

As the irradiation is ongoing, final conclusions cannot be made until the irradiation has finished and PIE of the test transducers and material samples is completed. However, some key observations about each task performed in this project can be noted.

First, the test capsule and instrumentation have operated as designed with the target irradiation temperature achieved. With the exception of the previously described sensitivity to temperature transients observed for the self powered detectors, the on-line measurement devices for temperature and the radiation fluxes (both gamma and neutron) have worked well. Finally, the results from on-line testing of the ultrasonic devices (both piezoelectric and magnetostrictive transducers) demonstrate that the devices are functioning with only minimal signal degradation due to thermal and irradiation effects. Preliminary analysis of the signals indicates that ultrasonic thermometry based on magnetostrictive devices is possible with materials similar to that included in the MITR irradiation. Furthermore, the irradiation behavior of the piezoelectric transducers demonstrates that on-line ultrasonic transducer measurements can be used for monitoring material behavior changes.

Signal processing will be an important element in using ultrasonic-based transducers to measure in-reactor behavior of nuclear fuel and material test specimens. The work to-date indicates that high resolution temperature measurements are possible with magnetostrictive thermometry. Improvements in the signal processing methods were noted, and it is recommended that additional measurement data be generated that can used to refine these methods.

Further work is required in three key areas: 1) continued acquisition and analysis of the on-line measurements from both the magnetostrictive and piezoelectric devices, 2) laboratory testing (including PIE) of the transducer materials and designs to understand the signal to noise ratio relationship to temperature effects, and 3) refinement of the signal processing procedures to further reduce the uncertainty in ultrasound-based sensor data. Although the first item and some of the second item will be completed using

ATR NSUF funding, a follow-on task is needed to ensure that all of the proposed last two activities are completed.

6. REFERENCES

1. J. Rempe, H. MacLean, R. Schley, D. Hurley, J. Daw, S. Taylor, J. Smith, J. Svoboda, D. Kotter, D. Knudson, S. C. Wilkins, M. Guers, L. Bond, L. Ott, J. McDuffee, E. Parma, and G. Rochau, *New In-Pile Instrumentation to Support Fuel Cycle Research and Development*, FCRD-FUEL-2011-000033 (also issued as INL/EXT-10-19149), January 2011.

2. C. Grandy, Argonne National Laboratory, personal communication to J. Rempe, Idaho National Laboratory, July 2012.

3. K. Natesan, M. Li, S. Majumdar, R.K. Nanstad, and T.-L. Sham, "Code Qualification of Structural Materials for AFCI Advanced Recycling Reactors," ANL-AFCI-244, September 2008.

4. *Light Water Reactor Sustainability Program Integrated Program Plan*, INL/EXT-11-23452, January 2012.

5. *Technical Program Plan for the Next Generation Nuclear Plant/Advanced Gas Reactor Fuel Development and Qualification Program*, PLN-3636, September 30, 2010.

6. *Summary for the Next Generation Nuclear Plant Project In Review*, INL/EXT-10-19142, Rev 1, September 2010.

7. *Next Generation Nuclear Plant Project Research and Development Status*, INL/EXT-10-19259, August 2010.

8. K. Natesan, S. Majumdar, P.S. Shankar, and V.N. Shah, "Preliminary Materials Selection Issues for the Next Generation Nuclear Plant Reactor Pressure Vessel," ANL/EXT-06/45, September 2006.

9. US Department of Energy, Office of Nuclera Energy, "Nuclear Energy Enabling Technologies Office of Nuclear Energy Advanced Sensors and Instrumentation Integrated Research Plan," September 2012.

10. K. Maeda, S. Sasaki, M. Kato, Y. Kihara. *J. Nucl. Mater.* 389 (2009) 78.

11. P. Millet, INL, *informal communication to J. Rempe, INL*, June 2010.

12. N. Chauvin, A. Courcelle, M. Pelletier, Y. Guerin, JM. Escleine, M. Phelip, F. Michel, S. Bejaoui, and M. Lainet, "Fuel Design, Irradiation Programme and Modelling, Application to Several Fuels for GENIV Systems," *presentation at 2010 ATR NSUF User's Week*, June 2010.

13. J. Daw, J. Rempe, P. Ramuhalli, R. Montgomery, H.T. Chien, B. Tittmann, B. Reinhardt, *NEET In-Pile Ultrasonic Sensor Enablement-FY 2012 Status Report*, INL/EXT-12-27233, September 2012.

14. J. Daw, J. Rempe, J. Palmer, P. Ramuhalli, R. Montgomery, H.T. Chien, B. Tittmann, B. Reinhardt, G. Kohse, *NEET In-Pile Ultrasonic Sensor Enablement-FY 2013 Status Report*, INL/EXT-13-29144, September 2013.

15. A. J. Palmer, G. L. McCormick, S. J. Corrigan, "Hydraulic Shuttle Irradiation System (HSIS) Recently Installed in the Advanced Test Reactor (ATR)," *Proceedings of ICAPP '10, Paper 10354*, San Diego, CA, USA, June 13-17, 2010

16. H.A. Tasman, M. Campana, D. Pel, J. Richter, "Ultrasonic Thin-Wire Thermometry for Nuclear Applications," *Temperature: Its Measurement and Control in Science and Industry,* Vol. 5, Part 2, pp. 1191-1196, 1982.

17. R.J. Grossman, "Ultrasonic-Thermometry Development for In-Situ Measurement of Nuclear-Fuel Temperatures (AWBA Development Program)," KAPL-4160, General Electric Company Knolls Atomic Power Laboratory, 1982.

18. E.P. Papdakis, L.C. Lynnworth, D.R. Patch, E.H. Carnevale, "Ultrasonic Thermometry in LMFBR Systems," Final Report NYO-3906-13, Panametrics Inc. 1972.

19. M. Laurie, D. Magallon, J. Rempe, S. Wilkins, J. Pierre, C. Marquié, S. Eymery, and R. Morice, "Ultrasonic High Temperature Sensors: Past Experiments and Prospective for Future Use," *International Journal of Thermophysics*, **31** (8-9): 1417-1427 Special Issue, September 2010.

20. J. F. Villard, "INSNU Project - Instrumentation for Irradiation Experiments in Research Reactors," *presentation at the Idaho National Laboratory*, Idaho Falls, ID, June 2008.

21. M. F. Narbey, D. Baron, G Despaux, JM Saurel, "Determination of the composition of a gas mixture in a nuclear fuel rod by an acoustic method," *Journal of the British Institute of Non-Destructive Testing (INSIGHT)*, **42**, 603-605 (2000).

22. J.Y. Ferrandis, G. Leveque, F. Augereau, E. Rosenkrantz, D. Baron, J-F. Villard, "An ultrasonic sensor for pressure and fission-gas release measurements in fuel rods for pressurised water reactors, *9th International conference on CANDU fuel*, Belleville (Canada), September 2005.

23. F. Augereau, J.-Y. Ferrandis, J.-F. Villard, D. Fourmentel, M. Dierckx, and J. Wagemans, "Effect of intense neutron dose irradiation on piezoceramics," *Transactions from Acoustics '08,* June 29-July 4, 2008, Paris, France.

24. D. Fourmentel, J. F. Villard, J. Y. Ferrandis, F. Augereau, E. Rosenkrantz, and M. Dierckx, "Acoustic Sensor for In-Pile Fuel Rod Fission Gas Release Measurement," *presented at ANIMMA Int. Conf.*, Marseille, June 7–10, 2009.

25. F. Algaber, JY. Ferrandis, F. Augereau, J-F. Villard, "PZT Materials under Gamma irradiation," *4th European Workshop on Piezoelectric Materials,* Montpellier (France), July 2004.

26. E. Rosenkrantz, J. Y. Ferrandis, F. Augereau, T. Lambert, D. Fourmentel, and X. Tiratay, "An Innovative Acoustic Sensor for First In-pile Fission Gas Release Determination - REMORA3 Experiment," *Proceedings of the Second International Conference on Advancements in Nuclear Instrumentation, Measurement Methods and their Applications (ANIMMA2011),* Ghent, Belgium, June 2011.

27. T. Lambert, E. Muller1, E. Federici1, E. Rosenkrantz, J.Y. Ferrandis, X. Tiratay, V. Silva, D. Machard, and G. Trillon, "REMORA 3: the fIrst Instrumented Fuel Experiment with On-line Gas Composition Measurement By Acoustic Sensor," *Proceedings of the Second International Conference on Advancements in Nuclear Instrumentation, Measurement Methods and their Applications (ANIMMA2011),* Ghent, Belgium, June 2011.

28. T. Lambert, E. Rosenkrantz, J.Y. Ferrandis, I. Zacharie-Aubrun, K. Hanifi, Ch. Valot, S. Reboul, and X. Tiratay, "Irradiation Behavior and Post-Irradiation Examinations of an Acoustic Sensor Using a Piezoelectric Transducer," *proceedings of the 2013 Conference on Advancements in Nuclear Instrumentation, Measurements Methods (ANIMMA 2013),* June 23-27, 2013, Marseilles, France.

29. D. Petti, INL, informal communication to J. Rempe, INL, July 27, 2012.

30. J. Rempe, D. Knudson, J. Daw, T. Unruh, B. Chase, K. Davis, and R. Schley, "New Instrumentation for Irradiation Testing in High Flux Materials and Test Reactors," *8th International Topical Meeting on Nuclear Plant Instrumentation, Control, and Human Machine Interface Technologies (NPIC&HMIT 2012),* San Diego, CA, July 22-26, 2012.

31. D. Ensminger, and L. J. Bond, *Ultrasonics: Fundamentals, Technologies, and Applications*, CRC Press, 2012.

32. K. Phani, et. al, "Estimation of Elastic Properties of Nuclear Fuel Material Using Longitudinal Ultrasonic Velocity - A New Approach," *J. Nucl. Mat.*, 366, 2007, pp. 129-136.

33. J. F. Villard, et. al.,"Acoustic Sensor for In-Pile Fuel Rod Fission Gas Release Measurement," *IEEE Transactions on Nuclear Science*, 58, 2011, pp. 151-155.

34. L.C. Lynnworth, "Ultrasonic Measurements for Process Control: Theory, Techniques, and Applications," Academic Press, 1989.

35. *MITR Users Guide Rev. 3 July 2012,* Massachusetts Institute of Technology (2012).

36. N. Gopalsami, A.C. Raptis, "Acoustic Velocity and Attenuation Measurements in Thin Rods with Application to Temperature Profiling in Coal Gasification Systems," *IEEE Transactions on Sonics and Ultrasonics*, SU-31, 1984, pp. 32-39.

37. K. E. Holbert, S. Sankaranarayanan, S. S. McCready, "Response of Lead Metaniobate Acoustic Emission Sensors to Gamma Irradiation," I*EEE Transactions on Nuclear Science*, vol. 52, no. 6, 2005, pp. 2583-2590.

38. Kulikov, et al., "Computer simulation of ferroelectric property changes in PLZT ceramics under neutron irradiation," *Proceedings of SPIE*, 4348, 2001, pp. 264-269.

39. H. Shea, "Radiation sensitivity of microelectromechanical system devices," *J. Micro/Nanolith.,* 8, 2009, pp. 1-11.

40. Wittels & Sherrill, "Fast Neutron Effects in Tetragonal Barium Titanate," J*ournal of Applied Physics*, 28 [5], 1957, pp. 606-609.

41. W. Primak, T. Anderson, "Metamimictization of Lithium Niobate by Thermal Neutrons," *Nuclear Technology*, 23, 1975, pp. 235.

42. T.K. Bierney, "Instrumentation for the Measurement of Vibration in Severe Environments Such as Nuclear Reactors," Endevco Technical Paper 272, 1976, pp. 1-8.

43. D.A. Parks, B. R. Tittmann. "Ultrasonic NDE in a Reactor Core," *Presented at Review of Progress in Quantitative Nondestructive Evaluation*, July 17-22, Burlington, VT, 2011.

44. R. Kazys, V. Voleisis, R. Sliteris, B. Voleisiene, L. Mazeika, and H. Abderrahim, "Research and Development of Radiation Resistant Ultrasonic Sensors for Quasi-Image Forming Systems in a Liquid Lead-Bismuth." *Ultragarsas (Ultrasound)*, 62(3),2006, pp. 7-15.

45. N. D. Patel, and P. S. Nicholson, "High Frequency - High Temperature Ultrasonic Transducers," *NDT International*, pp. 262-266, 1990.

46. D. Stubbs, and R. Dutton , "High-Temperature Ultrasonic Sensor for in Situ Monitoring of Hot Isostatic Processing," *SPIE*, 1996, pp. 164-172

47. K. Trachenko, "Understanding resistance to amorphization by radiation damage," *Journal of Physics: Condensed Matter*, 16(49), 2004, pp. R1491-R1515.

48. T. Yano, K. Inokuchi , M. Shikama , and J. Ukai, "Neutron irradiation effects on isotope tailored aluminum nitride ceramics by a fast reactor up to $2 \cdot l0^{26}$ n/m^2," *Journal of Nuclear Materials* , 2004, pp. 1471-1475.

49. Y. Ito, et al., "Radiation Damage of Materials Due to High Energy Ion Irradiation," *Nuclear Instruments and Methods in Physics Research*, 530, 2002

50. Y. P. Meleshko, S. G. Karpechko, G. K. Leont'ev, V. I. Nalivaev, A. D. Nikiforov, and V. M. , "Radiation Resistance of the Piezoelectric Ceramics TrsTS-21 and TNV-I," Translated from *Atomnaya Energiya*, 1986, pp. 50-52.

51. Evaluated Nuclear Data File (ENDF), Database Version of March 14, 2014, https://www-nds.iaea.org/exfor/endf00a.htm, Previous version accessed 2012.

52. L.C. Lynnworth, E.H. Carnevale, M.S. McDonough, S.S. Fam, "Ultrasonic Thermometry for Nuclear Reactors," *IEEE Transactions on Nuclear Science*, Vol. NS-16, pp. 184-187, 1968.

53. L.C. Lynnworth, "Nuclear Reactor Thermometry," US Patent Application 3,597,316: 3 Aug 1971.

54. S.C. Rogers, G.N. Miller., "Ultrasonic Level, Temperature, and Density Sensor," *IEEE Trans. on Nuclear Science*, 29 (1), 1982, pp. 665-668.

55. J. Daw, J. Rempe, S. Taylor, J. Crepeau, and S.C. Wilkins., "Ultrasonic Thermometry for In-Pile Temperature Detection," *Proceedings of NPIC&HMIT 2010*, 2010.

56. "What is Galfenol?", Etrema Products, Inc., http://www.etrema-usa.com/core/galfenol/, Accessed 08/09/2012.

57. Arnokrome 3 Datasheet Rev. 01-11-11,www.arnoldmagnetics.com/WorkArea/DownloadAsset.aspx?id=5262, Accessed 08/09/2012.

58. Arnokrome 4 Specification Rev. 1/11/11,www.arnoldmagnetics.com/WorkArea/DownloadAsset.aspx?id=5263, Accessed 08/09/2012.

59. Arnokrome 5 Specification Rev. 2/24/11,www.arnoldmagnetics.com/WorkArea/DownloadAsset.aspx?id=5328, Accessed 08/09/2012.

60. L. Barbot, CEA, *informal communication to J. Daw, J. Rempe, J. Palmer, B. Chase, INL*, G. Kohse, D. Carpenter, MIT, June 2014.

61. J. Sterbentz, INL, *informal communication to J. Daw, J. Rempe, J. Palmer, B. Chase, INL*, July 2014.

62. J. Daw, J. Rempe, J. Crepeau., "Update On Ultrasonic Thermometry Development at Idaho National Laboratory," *Proceedings of NPIC&HMIT 2012*, 2012.